SIAM J. Appl. Math.
Vol. 63, No. 4, pp. 1141–1183


# OPTIMIZATION OF ACOUSTIC SOURCE STRENGTH IN THE PROBLEMS OF ACTIVE NOISE CONTROL*

J. LONČARIĆ† AND S. V. TSYNKOV‡

**Abstract.** We consider a problem of eliminating the unwanted time-harmonic noise on a predetermined region of interest. The desired objective is achieved by active means, i.e., by introducing additional sources of sound called control sources, which generate the appropriate annihilating acoustic signal (antisound). A general solution for the control sources has been obtained previously in both continuous and discrete formulation of the problem. In the current paper, we focus on optimizing the overall absolute acoustic source strength of the control sources. Mathematically, this amounts to the minimization of multivariable complex-valued functions in the sense of $L_1$ with conical constraints, which are only "marginally" convex. The corresponding numerical optimization problem appears very challenging even for the most sophisticated state-of-the-art methodologies, and even when the dimension of the grid is small and the waves are long.

Our central result is that the global $L_1$-optimal solution can, in fact, be obtained without solving the numerical optimization problem. This solution is given by a special layer of monopole sources on the perimeter of the protected region. We provide a rigorous proof of global $L_1$ minimality for both continuous and discrete optimization problems in the one-dimensional case. We also provide numerical evidence that corroborates our result in the two-dimensional case, when the protected domain is a cylinder. Even though we cannot fully justify it, we believe that the same result holds in the general case, i.e., for multidimensional settings and domains of arbitrary shape. We formulate this notion as a conjecture at the end of the paper.

**Key words.** noise cancellation, control sources, minimization of amplitude, volume velocity, surface monopoles

**AMS subject classifications.** 35J05, 35C15, 35B37, 49J20, 65N06, 76Q05, 90C25, 90C30

**PII.** S0036139902404220

## 1. Introduction.

The area of active control of sound has a rich history of development, both as a chapter of theoretical acoustics and in the perspective of many different applications. Any attempt to adequately overview this extensive area in the framework of a focused research publication would obviously be deficient. Therefore, we simply refer the reader to monographs [3, 5, 11] that, among other things, contain a detailed survey of the literature.

The formulation of the problem that we use in the current paper has been introduced and studied in our previous work [7]; here, we analyze this formulation from the standpoint of optimization. Let $\Omega$ be a given domain, $\Omega \subset \mathbb{R}^n$, where the space dimension $n = 2$ or $n = 3$. (These two cases are most interesting for applications.) The domain $\Omega$ can be either bounded or unbounded; for reasons of simplicity we will further assume that $\Omega$ is bounded. Let $\Gamma$ be the boundary of $\Omega$: $\Gamma = \partial\Omega$. Both on $\Omega$ and on its (unbounded) complement $\Omega_1 = \mathbb{R}^n \backslash \Omega$ we consider the time-harmonic acoustic

*Received by the editors March 18, 2002; accepted for publication (in revised form) September 16, 2002; published electronically March 26, 2003. This research was supported by the National Aeronautics and Space Administration under NASA contract NAS1–97046, and in the framework of the Creativity and Innovation Program (C&I) while the authors were in residence at ICASE, NASA Langley Research Center.

http://www.siam.org/journals/siap/63-4/40422.html

†ICASE, MS 132C, NASA Langley Research Center, Hampton, VA 23681–2199. Current address: National Institute of Aerospace, 144 Research Drive, Hampton, VA 23666 (josip@nianet.org).

‡Department of Mathematics, North Carolina State University, Box 8205, Raleigh, NC 27695 and School of Mathematical Sciences, Tel Aviv University, Ramat Aviv, Tel Aviv 69978, Israel (tsynkov@math.ncsu.edu, http://www.math.ncsu.edu/∼stsynkov/).

field $u = u(\boldsymbol{x})$, $\boldsymbol{x} \in \mathbb{R}^n$, governed by the nonhomogeneous Helmholtz equation:

$$\boldsymbol{L}u \equiv \Delta u + k^2 u = f. \tag{1.1}$$

Equation (1.1) is subject to the Sommerfeld radiation boundary conditions at infinity, which for $n = 2$ are formulated as

$$u(\boldsymbol{x}) = O(|\boldsymbol{x}|^{-1/2}), \quad \frac{\partial u(\boldsymbol{x})}{\partial |\boldsymbol{x}|} + iku(\boldsymbol{x}) = o(|\boldsymbol{x}|^{-1/2}) \quad \text{as} \quad |x| \longrightarrow \infty, \tag{1.2a}$$

and for $n = 3$ as

$$u(\boldsymbol{x}) = O\left(|\boldsymbol{x}|^{-1}\right), \quad \frac{\partial u(\boldsymbol{x})}{\partial |\boldsymbol{x}|} + iku(\boldsymbol{x}) = o\left(|\boldsymbol{x}|^{-1}\right) \quad \text{as} \quad |\boldsymbol{x}| \longrightarrow \infty. \tag{1.2b}$$

The Sommerfeld boundary conditions specify the direction of wave propagation and distinguish between the incoming and outgoing waves at infinity by prescribing the outgoing direction only; they guarantee the unique solvability of the Helmholtz equation (1.1) for any compactly supported right-hand side $f = f(\boldsymbol{x})$. We define $\operatorname{supp} f = \{\boldsymbol{x} | f(\boldsymbol{x}) \neq 0\}$.

The source terms $f = f(\boldsymbol{x})$ in (1.1) can be located on both $\Omega$ and its complement $\Omega_1 = \mathbb{R}^n \backslash \Omega$; to emphasize the distinction, we define

$$f = f^+ + f^-, \tag{1.3}$$

where the sources $f^+$ are interior, $\operatorname{supp} f^+ \subset \Omega$, and the sources $f^-$ are exterior, $\operatorname{supp} f^- \subset \Omega_1$, with respect to $\Omega$. Accordingly, the overall acoustic field $u = u(\boldsymbol{x})$ can be represented as the sum of two components:

$$u = u^+ + u^-, \tag{1.4}$$

where

$$\boldsymbol{L}u^+ = f^+, \tag{1.5a}$$

$$\boldsymbol{L}u^- = f^-. \tag{1.5b}$$

Note that both $u^+ = u^+(\boldsymbol{x})$ and $u^- = u^-(\boldsymbol{x})$ are defined on the entire $\mathbb{R}^n$; the superscripts "+" and "−" refer to the sources that drive each of the field components, rather than to the domains of these components. The setup described above is schematically shown in Figure 1.1.

Hereafter, we will call the component $u^+$ of (1.4), (1.5a) *sound*, or the "friendly" part of the total acoustic field; the component $u^-$ of (1.4), (1.5b) will accordingly be called *noise*, or the "adverse" part of the total acoustic field. In the formulation that we are presenting, $\Omega$ will be a (predetermined) region of space to be shielded. This means that we would like to eliminate the noise inside $\Omega$ while leaving the sound component there unaltered. In the mathematical framework that we have adopted, the component $u^-$ of the total acoustic field, i.e., the response to the adverse sources $f^-$ (see (1.3), (1.4), (1.5)), will have to be cancelled on $\Omega$, whereas the component $u^+$, i.e., the response to the friendly sources $f^+$, will have to be left unaffected on $\Omega$. A physically more involved but conceptually easy-to-understand example can be given to illustrate the foregoing idea of shielding: inside the passenger compartment of an aircraft we would like to eliminate the noise coming from the propulsion system

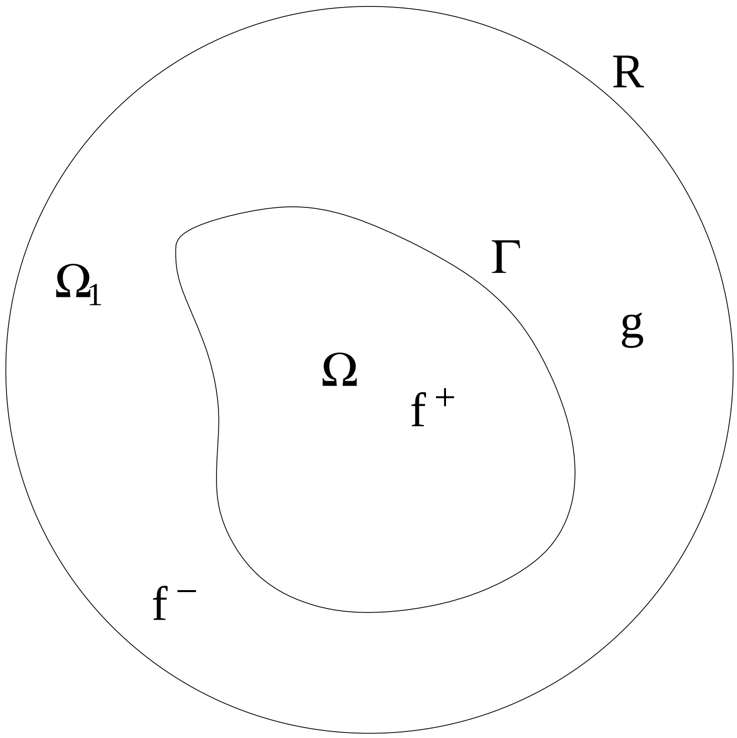


FIG. 1.1. *Geometric setup.*

located outside the fuselage, while not interfering with the ability of the passengers to listen to the in-flight entertainment programs or to converse.

The concept of *active noise control* that we will be discussing implies that the component $u^-$ is to be suppressed on $\Omega$ by introducing additional sources of sound $g = g(\boldsymbol{x})$ exterior with respect to $\Omega$, $\operatorname{supp} g \subset \Omega_1$, so that the total acoustic field $\tilde{u} = \tilde{u}(\boldsymbol{x})$ can now be governed by the equation (cf. formulae (1.1), (1.3))

$$\boldsymbol{L}\tilde{u} = f^+ + f^- + g \tag{1.6}$$

and coincide with only the friendly component $u^+$ on the domain $\Omega$:

$$\tilde{u}|_{\boldsymbol{x}\in\Omega} = u^+|_{\boldsymbol{x}\in\Omega}. \tag{1.7}$$

The new sources $g = g(\boldsymbol{x})$ of (1.6)—see Figure 1.1—will hereafter be referred to as the *control sources* or simply *controls.* An obvious solution for these control sources is $g = -f^-$. This solution, however, is excessively expensive. One one hand, the excessiveness comes from the information-type considerations, as the solution $g = -f^-$ requires explicit and detailed knowledge of the structure and location of the sources $f^-$. As shown in [7], this knowledge is, in fact, superfluous. On the other hand, the implementation of the solution $g = -f^-$ may encounter most serious technical difficulties. In the example above, it is obviously not feasible to directly counter the actual noise sources, which are aircraft propellers or turbofan jet engines located on, or underneath, the wings. Therefore, solutions of this noise control problem other than the most obvious one may be preferable from both the theoretical and practical standpoints. The general solution for the control sources $g$ was obtained in our previous work [7], and we describe it in section 2.

Before proceeding, let us note only that in the current paper we focus on the case of the standard constant-coefficient Helmholtz equation (1.1), which governs the acoustic field and is valid throughout the entire space $\mathbb{R}^n$. This allows us to make subsequent analysis most straightforward. As a matter of fact, other, more complex, cases that involve variable coefficients and possibly nonlinearities in the governing equations over some regions, as well as different types of far-field behavior, discontinuities in the material properties, etc., can be considered as well. Approaches to obtaining solutions for active controls in these cases are outlined in our previous paper [7] for the continuous formulation of the problem, and in the monograph by Ryaben'kii [15, Part VIII] for the discrete formulation of the problem.

The material in the rest of the paper is organized as follows. In section 2, we introduce the control sources for the continuous formulation of the problem. In section 3, we obtain the control sources in the discrete formulation of the problem, i.e., on the grid. In section 4, we discuss minimization of the overall acoustic source strength of active controls that we have constructed, which mathematically amounts to the optimization in the sense of $L_1$. We present convincing two-dimensional numerical evidence, as well as a rigorous one-dimensional proof, of the global $L_1$-optimality of a particular layer of monopole sources concentrated on the perimeter of the protected region. We believe that the combination of computations in two space dimensions and general proof in one space dimension cannot be a mere coincidence. As such, even though we cannot fully justify it, we formulate the corresponding general result on global $L_1$-optimality of surface monopoles as a conjecture in the concluding section 5. This conjecture basically implies that the aforementioned $L_1$-optimization problem can be solved without using any numerical optimization techniques.

## 2. Continuous control sources.

**2.1. General solution.** As demonstrated in [7], the general solution for the control sources $g = g(\boldsymbol{x})$ is given by the following formula ($\Omega_1 = \mathbb{R}^n \backslash \Omega$):

$$g(\boldsymbol{x}) = -\boldsymbol{L}w\Big|_{\boldsymbol{x}\in\Omega_1}, \tag{2.1}$$

where $w = w(\boldsymbol{x})$, $\boldsymbol{x} \in \Omega_1$, is a special auxiliary function-parameter that parameterizes the family of controls (2.1). The requirements that the function $w(\boldsymbol{x})$ must meet are, in fact, relatively "loose." At infinity, it has to satisfy the Sommerfeld boundary conditions (1.2a) or (1.2b). At the interface $\Gamma$, the function $w$ and its normal derivative have to coincide with the corresponding quantities that pertain to the total acoustic field $u$ given by formula (1.4):[1]

$$w\Big|_{\Gamma} = u\Big|_{\Gamma}, \qquad \frac{\partial w}{\partial \boldsymbol{n}}\Big|_{\Gamma} = \frac{\partial u}{\partial \boldsymbol{n}}\Big|_{\Gamma}. \tag{2.2}$$

Other than that, the function $w(\boldsymbol{x})$ used in (2.1) is arbitrary, and consequently formula (2.1) defines a large family of control sources, which, as will be seen in section 4, provides ample room for optimization. To make the discussion in the current paper

[1] In practice, the quantities $u$ and $\frac{\partial u}{\partial \boldsymbol{n}}$ on $\Gamma$ can be measured and supplied to the control system as the input data.

self-contained, we briefly outline below the justification for formula (2.1) as a general solution for controls, while referring the reader to [7] for further detail.

Introducing the fundamental solution $G = G(\boldsymbol{x})$ of the Helmholtz operator $\boldsymbol{L}$ of (1.1) for $n = 2$,

$$G(\boldsymbol{x}) = -\frac{1}{4i} H_0^{(2)}(k|\boldsymbol{x}|), \tag{2.3a}$$

where $H_0^{(2)}(z) = J_0(z) - iY_0(z)$ is the Hankel function of the second kind, and for $n = 3$,

$$G(\boldsymbol{x}) = -\frac{e^{-ik|\boldsymbol{x}|}}{4\pi|\boldsymbol{x}|}, \tag{2.3b}$$

we can obviously represent the sound portion $u^+ = u^+(\boldsymbol{x})$ of the overall acoustic field that satisfies (1.5a) everywhere on $\mathbb{R}^n$ as follows:

$$u^+(\boldsymbol{x}) = \int_\Omega G(\boldsymbol{x}-\boldsymbol{y}) f^+(\boldsymbol{y}) d\boldsymbol{y} = \int_\Omega G(\boldsymbol{x}-\boldsymbol{y}) \boldsymbol{L} u^+(\boldsymbol{y}) d\boldsymbol{y}, \quad \boldsymbol{x} \in \mathbb{R}^n. \tag{2.4}$$

Consequently, applying the classical Green's formula (see, e.g., [18] or [24]) to the function $u^+ = u^+(\boldsymbol{x})$ on $\Omega$, we have

$$\int_\Gamma \left( u^+ \frac{\partial G}{\partial \boldsymbol{n}} - \frac{\partial u^+}{\partial \boldsymbol{n}} G \right) ds_{\boldsymbol{y}} = 0, \quad \boldsymbol{x} \in \Omega, \tag{2.5}$$

where integrals in (2.5) are, again, convolutions. Similarly, applying the same Green's formula on $\Omega$ to $u^- = u^-(\boldsymbol{x})$ and using (2.5), we obtain

$$u^-(\boldsymbol{x}) = \int_\Gamma \left( u^- \frac{\partial G}{\partial \boldsymbol{n}} - \frac{\partial u^-}{\partial \boldsymbol{n}} G \right) ds_{\boldsymbol{y}} = \int_\Gamma \left( u \frac{\partial G}{\partial \boldsymbol{n}} - \frac{\partial u}{\partial \boldsymbol{n}} G \right) ds_{\boldsymbol{y}}, \quad \boldsymbol{x} \in \Omega. \tag{2.6}$$

Therefore, from (2.6) we can conclude that the desired annihilating acoustic signal $v = v(\boldsymbol{x})$ that cancels out the unwanted noise on $\Omega$ can be obtained as

$$v(\boldsymbol{x}) = -\int_\Gamma \left( u \frac{\partial G}{\partial \boldsymbol{n}} - \frac{\partial u}{\partial \boldsymbol{n}} G \right) ds_{\boldsymbol{y}}, \tag{2.7}$$

so that for $\boldsymbol{x} \in \Omega$ we indeed have

$$[u(\boldsymbol{x}) + v(\boldsymbol{x})]_{\boldsymbol{x}\in\Omega} = u^+(\boldsymbol{x}).$$

To actually implement the annihilating signal $v$ of (2.7), we introduce the auxiliary function $w = w(\boldsymbol{x})$ on $\mathbb{R}^n$ that satisfies the aforementioned conditions at the interface $\Gamma$ and at infinity, and apply the Green's formula to $w$, which yields

$$w(\boldsymbol{x}) - \int_\Omega G \boldsymbol{L} w d\boldsymbol{y} = \int_\Gamma \left( w \frac{\partial G}{\partial \boldsymbol{n}} - \frac{\partial w}{\partial \boldsymbol{n}} G \right) ds_{\boldsymbol{y}}, \quad \boldsymbol{x} \in \Omega. \tag{2.8}$$

As $w(\boldsymbol{x})$ satisfies the Sommerfeld conditions (1.2a) or (1.2b), we obviously have $w(\boldsymbol{x}) = \int_{\mathbb{R}^n} G \boldsymbol{L} w d\boldsymbol{y}$, $\boldsymbol{x} \in \mathbb{R}^n$, which, along with formulae (2.2) and (2.7), allows us to transform equality (2.8) to

$$v(\boldsymbol{x}) = -\int_{\Omega_1} G \boldsymbol{L} w d\boldsymbol{y}. \tag{2.9}$$

Equation (2.9) implies that for any $w = w(\boldsymbol{x})$ chosen as described above, formula (2.1) describes an appropriate control function.

Conversely, assume that $g = g(x)$, $\operatorname{supp} g \subset \Omega_1$, is a control field such that the solution $\tilde{u} = \tilde{u}(\boldsymbol{x})$ of (1.6) subject to the Sommerfeld conditions (1.2a) or (1.2b) satisfies equality (1.7). Then, by choosing $w = w(\boldsymbol{x})$, $\boldsymbol{x} \in \mathbb{R}^n$, as the solution to the nonhomogeneous equation

$$-\boldsymbol{L}w = g - f^+,$$

subject to the corresponding Sommerfeld condition, (1.2a) or (1.2b), one can represent $g$ in the form (2.1); see [7]. Altogether, we obtain that formula (2.1) describes the general solution for controls. In other words, for any $w(\boldsymbol{x})$, formula (2.1) provides an appropriate control field $g(\boldsymbol{x})$, and any appropriate control field $g(\boldsymbol{x})$ can be represented in the form (2.1) with some particular choice of $w(\boldsymbol{x})$.

Let us emphasize several important properties of controls (2.1). First of all, from the foregoing derivation we can see that to obtain these controls one needs no knowledge of the actual exterior sources of noise $f^-$. In other words, neither their location, nor structure, nor strength are required. All one needs to know is $u$ and $\frac{\partial u}{\partial \boldsymbol{n}}$ on the perimeter $\Gamma$ of the protected region $\Omega$. As has been mentioned, in a practical setting $u|_\Gamma$ and $\frac{\partial u}{\partial \boldsymbol{n}}|_\Gamma$ can be interpreted as measurable quantities that are supplied to the control system as the input data. Moreover, these measurable quantities refer to the overall acoustic field $u$, rather than only to its unwanted component $u^-$. In other words, the methodology can automatically distinguish between the signals coming from the exterior and interior sources, and can tune the controls so that they cancel only the unwanted exterior signal. This capability is extremely important, as in many applications the overall acoustic field always contains a component that needs to be suppressed along with the part that needs to be left intact. Alternatively, one can say that the control sources (2.1) are insensitive to the interior sound $u^+(\boldsymbol{x})$. Indeed, given a function $w(\boldsymbol{x})$ that satisfies interface conditions (2.2) and the radiation boundary conditions at infinity, we can take instead $\tilde{w}(\boldsymbol{x}) = w(\boldsymbol{x}) - u^+(\boldsymbol{x})$; this new function will satisfy the interface conditions (2.2) with $u$ replaced by $u^-$ and the same Sommerfeld conditions at infinity. Most important, the control sources generated by $\tilde{w}(\boldsymbol{x})$ will be the exact same control sources as those generated by $w(\boldsymbol{x})$ because $\boldsymbol{L}\tilde{w}(\boldsymbol{x}) = \boldsymbol{L}[w(\boldsymbol{x}) - u^+(\boldsymbol{x})] = \boldsymbol{L}w(\boldsymbol{x})$ for $\boldsymbol{x} \in \Omega_1$.

Let us also note that in a more general framework, formula (2.9) (with (2.2) taken into account) can be interpreted as a particular case of the generalized potential of Calderon's type with the vector density $-\big(u, \frac{\partial u}{\partial \boldsymbol{n}}\big)|_\Gamma$. This more general framework allows us to analyze more complex formulations of the active noise control problem (see [7]) such as those that involve variations in material properties and alternative types of far-field behavior of the solution. We refer the reader to the original work by Calderon [2] and Seeley [16], as well as to the monograph by Ryaben'kii [15], for general concepts related to Calderon's potentials and associated pseudodifferential boundary projection operators. As concerns the aforementioned more advanced formulations of the noise control problem, the key result is basically the same as above. The general solution for control sources is still given by formula (2.1), where the auxiliary function $w(\boldsymbol{x})$ should still satisfy the interface conditions (2.2) and the problem-specific far-field boundary conditions (in case they differ from the previously mentioned Sommerfeld conditions). The operator $\boldsymbol{L}$ in formula (2.1) will, however, no longer be the constant-coefficient Helmholtz operator of (1.1); it will rather be the problem-specific variable-coefficients operator that accounts for the particular variations in material properties, etc. However, since formula (2.1) for controls does not change (see [7]), we immediately conclude that we, in fact, do not need to know the operator $\boldsymbol{L}$ on $\Omega$. In other words, for obtaining the control sources we do not need to know the material properties of the sound-conducting medium inside the protected region. This result (see [7]), which at first seems counterintuitive, has, in fact, a straightforward physical explanation. We only need to realize that the noise we want to suppress, and the output of controls that is supposed to annihilate this noise, propagate across one and the same medium, and we do not need to know what this medium is (under some relatively nonrestrictive limitations; see [7]). It is also interesting to mention that the aforementioned Calderon boundary projection operators essentially render the decomposition of the wave field $u(\boldsymbol{x})$ on the boundary $\Gamma$ into its incoming and outgoing component with respect to the domain $\Omega$; see [7]. Subsequently, the controls (2.1) can be interpreted as either sources cancelling the incoming wave field for the domain to be shielded, i.e., $\Omega$, or alternatively, as sources cancelling the outgoing wave field for the domain complementary to the one to be shielded, i.e., $\Omega_1 = \mathbb{R}^n \backslash \Omega$. The latter interpretation is often more versatile; see [7].

Another important thing to notice is that the control sources $g(\boldsymbol{x})$ of (2.1) are defined, generally speaking, on the entire complementary domain $\Omega_1 = \mathbb{R}^n \backslash \Omega$. For the analysis of specific problems, especially when the protected region $\Omega$ is bounded and the complementary region $\Omega_1$ is unbounded, as in Figure 1.1, it may be convenient to consider compactly supported control sources, i.e., the control sources concentrated in the vicinity of the interface $\Gamma$. To obtain such controls, one needs to narrow down the class of functions $w(\boldsymbol{x})$ used in formula (2.1). Namely, instead of considering arbitrary $w(\boldsymbol{x})$ subject only to constraints (2.2) and Sommerfeld boundary conditions at infinity, one needs to consider $w(\boldsymbol{x})$ that become a solution to the homogeneous Helmholtz equation everywhere outside some larger domain that fully contains the protected region $\Omega$. In so doing, the area outside $\Omega$ that supports the controls $g(\boldsymbol{x})$ of (2.1) will stretch from $\Gamma$ to the outer boundary of the aforementioned larger domain, and may basically look like a curvilinear strip adjacent to $\Gamma$ from the exterior side. This strip may, in principle, be made as narrow as desired and may eventually shrink completely, thus reducing to only the interface $\Gamma$ itself. As will be seen, the sources $g(\boldsymbol{x})$ supported only on the perimeter $\Gamma$ represent an important class of active controls. Such distributions $g(\boldsymbol{x})$ include monopole and dipole layers as special cases, which are idealizations of pulsating or vibrating membranes.

**2.2. Artificial boundary conditions and compactly supported controls.** To actually obtain compactly supported controls $g(\boldsymbol{x})$ in a particular setting, it is often convenient to use the methodology known as artificial boundary conditions (see the review paper [19]) for the selection of the appropriate function $w(\boldsymbol{x})$ in formula (2.1). Assume that $w(\boldsymbol{x})$ satisfies the homogeneous Helmholtz equation $\boldsymbol{L}w = 0$ outside some outer artificial boundary, which is a closed surface (curve) with an interior that fully contains $\Omega$. In Figure 1.1, we schematically represent this outer boundary as a sphere (circle) of radius $R$. It turns out that one can equivalently replace the homogeneous equation $\boldsymbol{L}w = 0$ along with the Sommerfeld boundary conditions at infinity by the special artificial boundary conditions (ABCs) at the outer boundary. For the outer boundary of a general shape, this can be done most efficiently using the same apparatus of Calderon's pseudodifferential boundary projection operators (see [15, 19]) that has been mentioned before. For the particular case of a regular spherical or circular outer boundary (see Figure 1.1), which is convenient due to the simplicity of the analysis, the construction of the ABCs is described below. We emphasize that the forthcoming boundary conditions are exact. In other words, they are set at a finite artificial boundary and are fully equivalent to the Sommerfeld boundary conditions set at infinity. They also appear to be nonlocal. High accuracy (exactness) and nonlocality of the ABCs that we introduce and use hereafter present a notable distinction compared to many approximate methods, which are typically local but not as accurate; see, e.g., [19].

We will use spherical coordinates $(\rho, \theta, \phi)$ in $\mathbb{R}^n$, $n = 3$, and assume that $\boldsymbol{L}w = 0$ for $|\boldsymbol{x}| \equiv \rho \geq R$; see Figure 1.1. In addition, we will assume that $w(\boldsymbol{x})$ satisfies the Sommerfeld boundary condition (1.2b). Expanding $w(\boldsymbol{x})$ with respect to spherical functions $Y_l^m$, $l = 0, 1, 2, \dots$, $m = 0, \pm 1, \dots, \pm l$, and separating the variables in the differential operator $\boldsymbol{L}$, we arrive at the following collection of second-order ordinary differential equations:

$$\begin{gathered} \frac{d^2 \hat{w}_{lm}}{d\rho^2} + \frac{2}{\rho}\frac{d\hat{w}_{lm}}{d\rho} + \left[k^2 - \frac{l(l+1)}{\rho^2}\right]\hat{w}_{lm} = 0, \\ \rho \geq R, \quad l = 0, 1, 2, \dots, \quad m = 0, \pm 1, \dots, \pm l, \end{gathered} \tag{2.10}$$

for the unknown radial modes $\hat{w}_{lm}$. These modes are also supposed to satisfy boundary conditions at infinity

$$\hat{w}_{lm}(\rho) = O\left(\rho^{-1}\right), \quad \frac{d\hat{w}_{lm}(\rho)}{d\rho} + ik\hat{w}_{lm}(\rho) = o\left(\rho^{-1}\right) \quad \text{as} \quad \rho \longrightarrow \infty, \tag{2.11}$$

which immediately follow from the Sommerfeld condition (1.2b). For any given pair $(l, m)$ the general solution of (2.10) is given by

$$\hat{w}_{lm} = \frac{c_1}{\sqrt{\rho}} H^{(1)}_{l+1/2}(k\rho) + \frac{c_2}{\sqrt{\rho}} H^{(2)}_{l+1/2}(k\rho), \tag{2.12}$$

where $c_1$ and $c_2$ are arbitrary constants and $H^{(1)}_{l+1/2}(k\rho)$ and $H^{(2)}_{l+1/2}(k\rho)$ are Hankel functions of the first and second kind, respectively. Taking into account the asymptotic expressions for the Hankel functions for a fixed order $\nu$ and large values of $\rho$ (see, e.g., [24]),

$$\begin{aligned} H^{(1)}_\nu(\rho) &= \sqrt{\frac{2}{\pi\rho}} \exp\left[i\left(\rho - \frac{\pi}{2}\nu - \frac{\pi}{4}\right)\right] + O\left(\rho^{-3/2}\right), \\ H^{(2)}_\nu(\rho) &= \sqrt{\frac{2}{\pi\rho}} \exp\left[-i\left(\rho - \frac{\pi}{2}\nu - \frac{\pi}{4}\right)\right] + O\left(\rho^{-3/2}\right), \end{aligned}$$

we conclude that only $\rho^{-1/2} H^{(2)}_{l+1/2}(k\rho)$ satisfies boundary conditions (2.11), and consequently the constant $c_1$ (see (2.12)) in any particular solution that satisfies the Sommerfeld conditions at infinity has to be equal to zero. As the two functions $\rho^{-1/2} H^{(1)}_{l+1/2}(k\rho)$ and $\rho^{-1/2} H^{(2)}_{l+1/2}(k\rho)$ form a fundamental system of solutions for the linear homogeneous second-order ODE (2.10), requiring that only one of them, $\rho^{-1/2} H^{(2)}_{l+1/2}(k\rho)$, be present in the actual solution $\hat{w}_{lm}$ is equivalent to requiring that $\hat{w}_{lm}(\rho)$ be parallel to $\rho^{-1/2} H^{(2)}_{l+1/2}(k\rho)$ for $\rho \geq R$ in the sense of the corresponding Wronskian vanishing at $\rho = R$:

$$\det \left. \begin{bmatrix} \hat{w}_{lm} & \rho^{-1/2} H^{(2)}_{l+1/2}(k\rho) \\ \frac{d}{d\rho}\hat{w}_{lm} & \frac{d}{d\rho}\left(\rho^{-1/2} H^{(2)}_{l+1/2}(k\rho)\right) \end{bmatrix} \right|_{\rho=R} = 0. \tag{2.13}$$

Obviously, equality (2.13) enforced at $\rho = R$ implies that it will hold for all $\rho \geq R$ as well. Equality (2.13) is a linear homogeneous relation between a given Fourier component $\hat{w}_{lm}$ of the solution $w(\boldsymbol{x})$ and the corresponding Fourier component $\frac{d}{d\rho}\hat{w}_{lm}$ of its normal derivative $\frac{d}{d\rho}w(\boldsymbol{x})$ on the spherical surface $\rho = R$. The entire family of such relations for all $l = 0, 1, 2, \dots$ and $m = 0, \pm 1, \dots, \pm l$ set at $\rho = R$ is equivalent to saying that the function $w = w(\boldsymbol{x})$ originally defined inside the sphere, i.e., for $\rho \leq R$, can be smoothly extended to the region $\rho \geq R$ so that the extension will solve the homogeneous equation $\boldsymbol{L}w = 0$ for $\rho \geq R$ and have a proper far-field behavior, i.e, satisfy the Sommerfeld condition (1.2b). Hereafter, we will refer to relations (2.13) for $l = 0, 1, 2, \dots$ and $m = 0, \pm 1, \dots, \pm l$ as *the artificial boundary conditions* for the three-dimensional Helmholtz equation on the spherical surface $\rho = R$.

The ABCs for the two-dimensional case on the circular external artificial boundary $\rho = R$ can be obtained similarly. We introduce polar coordinates $(\rho, \theta)$ in $\mathbb{R}^n$, $n = 2$, use standard Fourier expansion in the circumferential direction with respect to the complex exponents $e^{-il\theta}$, $l = 0, \pm 1, \pm 2, \dots$, and arrive at the following collection of second-order ordinary differential equations:

$$\frac{d^2\hat{w}_l}{d\rho^2} + \frac{1}{\rho}\frac{d\hat{w}_l}{d\rho} + \left[k^2 - \frac{l^2}{\rho^2}\right]\hat{w}_l = 0, \quad \rho \geq R, \quad l = 0, \pm 1, \pm 2, \dots, \tag{2.14}$$

for the unknown radial modes $\hat{w}_l$. These modes are also supposed to satisfy boundary conditions at infinity

$$\hat{w}_l(\rho) = O(\rho^{-1/2}), \quad \frac{d\hat{w}_l(\rho)}{d\rho} + ik\hat{w}_l(\rho) = o(\rho^{-1/2}) \quad \text{as} \quad \rho \longrightarrow \infty, \tag{2.15}$$

which immediately follow from the Sommerfeld condition (1.2a). For every given $l$, (2.14) is the Bessel equation and has general solution

$$\hat{w}_l = c_1 H_l^{(1)}(k\rho) + c_2 H_l^{(2)}(k\rho), \tag{2.16}$$

where $c_1$ and $c_2$ are, again, arbitrary constants. The asymptotics of the Hankel functions for large $\rho$'s indicates that to satisfy (2.15) one must have $c_1 = 0$ in any particular solution that satisfies the radiation conditions at infinity. This requirement leads to the following ABCs for the two-dimensional Helmholtz equation:

$$\det \begin{bmatrix} \hat{w}_l & H_l^{(2)}(k\rho) \\ \frac{d}{d\rho}\hat{w}_l & \frac{d}{d\rho}H_l^{(2)}(k\rho) \end{bmatrix}\Bigg|_{\rho=R} = 0, \tag{2.17}$$

where relations (2.17) should be considered for all $l = 0, \pm 1, \pm 2, \dots$. We refer the reader to the review article [19] for further detail on the construction of ABCs for different equations in different settings. Let us also reiterate that once the ABCs (2.13) or (2.17) are satisfied for all radial modes, then we can consider $\boldsymbol{L}w = 0$ for $\rho \geq R$, and as such, the resulting control sources $g(\boldsymbol{x})$ given by (2.1) will be compactly supported between the interface $\Gamma$ and the external artificial boundary $\rho = R$.

**2.3. Types of control sources.** Let us now analyze the continuous control sources from the standpoint of their geometric location and the type of acoustic excitation that they provide. To put this analysis into a mathematical perspective, it will be convenient to use the apparatus of distributions; see, e.g., [24].

In our original derivation of formula (2.1), we have implicitly assumed that the function $w(\boldsymbol{x})$ was sufficiently smooth so that the operator $\boldsymbol{L}$ could be applied in the classical sense everywhere on $\Omega_1 = \mathbb{R}^n \backslash \Omega$. In this case, the function $g(\boldsymbol{x})$ is locally absolutely integrable, $g \in \boldsymbol{L}_1^{(\mathrm{loc})}(\Omega_1)$, and can be interpreted as a regular distribution. As for any other distribution, it can be represented as a convolution of its own self with the $\delta$-function: $g = \delta * g$. This means that from the mathematical standpoint the control field $g(\boldsymbol{x})$ can be viewed as an expansion in terms of the elementary point monopoles $g(\boldsymbol{y})\delta(\boldsymbol{x}-\boldsymbol{y})$ with regular density $g$:

$$g(\boldsymbol{x}) = \delta * g = \int_{\mathbb{R}^n} g(\boldsymbol{y})\delta(\boldsymbol{x}-\boldsymbol{y})d\boldsymbol{y}. \tag{2.18}$$

Next, we recall that, by definition of the fundamental solution $\boldsymbol{L}G = \delta(\boldsymbol{x})$, the response to every such elementary monopole $g(\boldsymbol{y})\delta(\boldsymbol{x}-\boldsymbol{y})$ will be given by $g(\boldsymbol{y})G(\boldsymbol{x}-\boldsymbol{y})$, and consequently, the overall control output

$$G * g = \int_{\mathbb{R}^n} g(\boldsymbol{y})G(\boldsymbol{x}-\boldsymbol{y})d\boldsymbol{y} \tag{2.19}$$

will be interpreted as superposition of the foregoing elementary responses, i.e., solutions generated by the aforementioned point monopoles. Altogether we see that the original formula (2.1) provides the general solution for controls in the class of regular distributions $\boldsymbol{L}_1^{(\mathrm{loc})}(\Omega_1)$, which corresponds to the volumetric control sources of monopole type on the complementary domain $\Omega_1 = \mathbb{R}^n \backslash \Omega$. Compactly supported controls discussed in section 2.2 obviously fall into this category. Later on we will see that this class of functions contains, in fact, all meaningful volumetric excitations.

In many cases it may also be desirable to consider surface controls, i.e., the control sources that are concentrated only on the interface $\Gamma$. Let us first assume that there are no interior sources, which means that $u^+(\boldsymbol{x}) = 0$, and the acoustic field we want to control consists only of its adverse component, $u(\boldsymbol{x}) \equiv u^-(\boldsymbol{x})$. After the control, the overall acoustic field has to be equal to zero on the domain $\Omega$. As shown in [20], the general solution for surface controls is given by

$$g^{(\mathrm{surf})} = -\left[\frac{\partial w}{\partial \boldsymbol{n}} - \frac{\partial u}{\partial \boldsymbol{n}}\right]_\Gamma \delta(\Gamma) - \frac{\partial}{\partial \boldsymbol{n}}\big([w-u]_\Gamma \delta(\Gamma)\big), \tag{2.20}$$

where $w = w(\boldsymbol{x})$, as before, denotes the auxiliary function-parameter that in this case has to satisfy the homogeneous Helmholtz equation on the complementary domain, $\boldsymbol{L}w = 0$ for $\boldsymbol{x} \in \Omega_1$, and the Sommerfeld boundary condition (1.2a) or (1.2b) at infinity. Expressions in rectangular brackets in formula (2.20) denote discontinuities of the corresponding quantities across the interface $\Gamma$. The first term on the right-hand side of (2.20) represents the density of a single-layer potential, which is a layer of monopoles on the interface $\Gamma$, and the second term on the right-hand side of (2.20) represents the density of a double-layer potential, which is a layer of dipoles on the interface $\Gamma$.

A detailed justification of formula (2.20) as general solution for surface controls can be found in [20]. Here we mention only that it basically amounts to proving that a given solution $u(\boldsymbol{x})$ of the homogeneous equation $\boldsymbol{L}u = 0$ on $\Omega$ can be represented as a combination of a single-layer potential and a double-layer potential if and only if the densities of the aforementioned potentials are defined as $\left[\frac{\partial w}{\partial \boldsymbol{n}} - \frac{\partial u}{\partial \boldsymbol{n}}\right]_\Gamma \delta(\Gamma)$ and

$\frac{\partial}{\partial \boldsymbol{n}}([w-u]_\Gamma \delta(\Gamma))$, respectively (cf. formula (2.20)). The direct implication is easy to establish by applying the operator $\boldsymbol{L}$ to the discontinuous function

$$v(\boldsymbol{x}) = \begin{cases} u(\boldsymbol{x}) & \text{for} \quad \boldsymbol{x} \in \Omega, \\ w(\boldsymbol{x}) & \text{for} \quad \boldsymbol{x} \in \Omega_1, \end{cases} \tag{2.21}$$

in the sense of distributions (see [24]), which yields

$$\boldsymbol{L}v = \left[\frac{\partial w}{\partial \boldsymbol{n}} - \frac{\partial u}{\partial \boldsymbol{n}}\right]_\Gamma \delta(\Gamma) + \frac{\partial}{\partial \boldsymbol{n}}\big([w-u]_\Gamma \delta(\Gamma)\big), \tag{2.22}$$

and subsequently reconstructing $u(\boldsymbol{x})|_{\boldsymbol{x}\in\Omega} = v(\boldsymbol{x})|_{\boldsymbol{x}\in\Omega}$ as a convolution with the fundamental solution. The inverse implication requires explicitly obtaining $w(\boldsymbol{x})$ for a given $u(\boldsymbol{x})$ and given surface densities, which is done in [20], again, in the form of a special surface integral. Then, the control sources (2.20) are obtained by simply taking (2.22) with the opposite sign, which guarantees the cancellation of $u(\boldsymbol{x})$ on $\Omega$ by $-v(\boldsymbol{x})$.

In the family of surface controls (2.20) we identify two important particular cases. First, the cancellation of $u(\boldsymbol{x})$, $\boldsymbol{x} \in \Omega$, can be achieved by using only the surface monopoles, i.e., by employing only a single-layer potential as the annihilating signal. To do that, we need to find $w(\boldsymbol{x})$, $\boldsymbol{x} \in \Omega_1$, such that the overall function $v(\boldsymbol{x})$ of (2.21) would have the discontinuity on $\Gamma$ only in its normal derivative and not in the function itself. This $w(\boldsymbol{x})$ will then be a solution of the following external Dirichlet problem:

$$\begin{gathered} \boldsymbol{L}w = 0, \quad \boldsymbol{x} \in \Omega_1, \\ w\big|_\Gamma = u\big|_\Gamma, \end{gathered} \tag{2.23}$$

subject to the appropriate Sommerfeld boundary condition (1.2a) or (1.2b). Problem (2.23) is always uniquely solvable on $\Omega_1 = \mathbb{R}^n \backslash \Omega$. Second, one can employ only the double-layer potential to cancel out $u(\boldsymbol{x})$, $\boldsymbol{x} \in \Omega$, i.e., use only surface dipoles as the control sources. In this case, the function $w(\boldsymbol{x})$, $\boldsymbol{x} \in \Omega_1$, has to be such that $v(\boldsymbol{x})$ given by (2.21) would have discontinuity on $\Gamma$ only in the function itself and not in its normal derivative. This $w(\boldsymbol{x})$ should then solve the following external Neumann problem:

$$\begin{gathered} \boldsymbol{L}w = 0, \quad \boldsymbol{x} \in \Omega_1, \\ \frac{\partial w}{\partial \boldsymbol{n}}\bigg|_\Gamma = \frac{\partial u}{\partial \boldsymbol{n}}\bigg|_\Gamma, \end{gathered} \tag{2.24}$$

again, subject to the appropriate Sommerfeld condition at infinity, (1.2a) or (1.2b); the latter guarantees the solvability of (2.24).

In a more general case, when interior sources are present, the results, in fact, do not change. Assume, as before, that the overall acoustic field is the sum of its friendly and adverse components (see (1.4)), $u(\boldsymbol{x}) = u^+(\boldsymbol{x}) + u^-(\boldsymbol{x})$, and we want to cancel out $u^-(\boldsymbol{x})$ on $\Omega$. Then, formula (2.20), where $u$ shall now be interpreted as in (1.4) and $w$ is a function-parameter, will still provide the general solution for surface controls. Indeed, since $\boldsymbol{L}u^+ = 0$ on $\Omega_1$ and, moreover, $u^+(x)$ and $\frac{\partial u^+}{\partial \boldsymbol{n}}(\boldsymbol{x})$ are continuous across the interface $\Gamma$, then (2.20) simply reduces to

$$g^{(\text{surf})} = -\left[\frac{\partial \tilde{w}}{\partial \boldsymbol{n}} - \frac{\partial u^-}{\partial \boldsymbol{n}}\right]_\Gamma \delta(\Gamma) - \frac{\partial}{\partial \boldsymbol{n}}\big([\tilde{w} - u^-]_\Gamma \delta(\Gamma)\big), \tag{2.25}$$

where the new function-parameter $\tilde{w}$ is given by $\tilde{w}(\boldsymbol{x}) = w(\boldsymbol{x}) - u^+(\boldsymbol{x})$ and, as such, satisfies the aforementioned general requirements of $w$'s. This means that the control sources $g^{(\text{surf})}(\boldsymbol{x})$, $\boldsymbol{x} \in \Gamma$, defined by (2.20), or equivalently (2.25), appear insensitive to the friendly component $u^+(\boldsymbol{x})$ of the acoustic field, and will precisely annihilate $u^-(\boldsymbol{x})$ on the domain $\Omega$. Furthermore, the entire family of surface controls (2.25) is obviously the exact same family as we would have obtained if there were no interior sources and the overall acoustic field consisted of only $u^-(\boldsymbol{x})$. It is also clear that the same reasoning will apply to the particular cases of purely monopole and purely dipole controls. Namely, if in problems (2.23) and (2.24) we interpreted the boundary data $u$ and $\frac{\partial u}{\partial \boldsymbol{n}}$ (respectively) in the sense of (1.4), then the solution $w$ of either problem would obviously be $w(\boldsymbol{x}) = \tilde{w}(\boldsymbol{x}) + u^+(\boldsymbol{x})$, where $\tilde{w}(\boldsymbol{x})$ is the solution that corresponds to $u^+(\boldsymbol{x}) \equiv 0$. This means that both the monopole and the dipole layers constructed using the respective solution $w(\boldsymbol{x})$ would be the exact same monopole or dipole layer that suppresses $u^-(\boldsymbol{x})$ on $\Omega$ in the case of no interior sources and no interior sound.

Altogether we conclude that, as indicated by formula (2.20), surface control sources are combinations of monopole and dipole layers, with the two "extreme" cases corresponding to either only monopoles (see (2.23)) or only dipoles (see (2.24)). From the standpoint of physics, the monopole and dipole sources provide different types of excitation to the surrounding sound-conducting medium. A point monopole source can be interpreted as a vanishingly small pulsating sphere that radiates acoustic waves symmetrically in all directions, whereas a point dipole source resembles a small oscillating membrane that has a particular directivity of radiation (see, e.g., [11] for a more detailed discussion on the properties of different sources). This distinction basically warrants a separate consideration of the monopole- and dipole-type sources as far as the pointwise or surface excitation may be concerned. However, in the context of volumetric excitation, a separate consideration of dipole fields appears, in effect, superfluous.

Indeed, a point dipole is characterized by its (complex) magnitude $b$ and direction $\boldsymbol{m}$ (cf. formula (2.20)):

$$-b\frac{\partial \delta}{\partial \boldsymbol{m}} = -b\langle \boldsymbol{m}, \nabla\delta\rangle = -\langle \boldsymbol{b}, \nabla\delta\rangle, \tag{2.26}$$

where the definition of $\nabla\delta$ is standard, i.e., for any test function $\phi \in \mathcal{D}$ we have $(\nabla\delta, \phi) = -(\delta, \nabla\phi) = -\nabla\phi(0)$, $\langle\cdot,\cdot\rangle$ denotes a conventional real scalar product, and the complex $n$-dimensional vector $\boldsymbol{b} \equiv b\boldsymbol{m}$ is called the dipole moment.[2] Let us now consider a volumetric distribution of dipoles, i.e., a right-hand side to the Helmholtz equation given in the following convolution form (cf. formula (2.18)):

$$b(\boldsymbol{x}) = -\int_{\mathbb{R}^n} \langle \boldsymbol{b}(\boldsymbol{y}), \nabla\delta(\boldsymbol{x}-\boldsymbol{y})\rangle d\boldsymbol{y} = -\sum_{i=1}^{n} b_i * \nabla_i\delta, \tag{2.27}$$

where $\boldsymbol{b}$ is a regular vector field. Since the convolution of any distribution with the $\delta$-function always exists [24], we can rewrite (2.27) as

$$b(\boldsymbol{x}) = -\sum_{i=1}^{n} \nabla_i b_i * \delta = -\int_{\mathbb{R}^n} \operatorname{div}\boldsymbol{b}(\boldsymbol{y})\delta(\boldsymbol{x}-\boldsymbol{y})d\boldsymbol{y} = -\operatorname{div}\boldsymbol{b} * \delta = -\operatorname{div}\boldsymbol{b}. \tag{2.28}$$

[2]We emphasize that $\boldsymbol{b}$ is not a most general complex vector, but rather a product of a single complex quantity $b$ and a real $n$-dimensional vector $\boldsymbol{m}$.

Formula (2.28) implies that if we additionally require that the vector field $\boldsymbol{b}(\boldsymbol{y})$ be somewhat more regular than simply $\boldsymbol{b} \in L_1^{(\mathrm{loc})}(\Omega_1)$, namely, $\mathrm{div}\boldsymbol{b} \in L_1^{(\mathrm{loc})}(\Omega_1)$, then the volumetric distribution of dipoles can be reduced to an equivalent volumetric distribution of monopoles as in (2.18).

Next, by differentiating the relation $\boldsymbol{L}G = \delta$, we obtain that the response to the point dipole excitation (2.26) is given by $-\langle \boldsymbol{b}, \nabla G \rangle$. Accordingly, the solution that corresponds to the distribution of sources (2.27) or (2.28) is given by (cf. formula (2.19))

$$
\begin{aligned}
u(\boldsymbol{x}) &= -\int_{\mathbb{R}^n} \langle \boldsymbol{b}(\boldsymbol{y}), \nabla G(\boldsymbol{x}-\boldsymbol{y})\rangle d\boldsymbol{y} = -\sum_{i=1}^{n} b_i * \nabla_i G \\
&= -\sum_{i=1}^{n} \nabla_i b_i * G = -\int_{\mathbb{R}^n} \mathrm{div}\boldsymbol{b}(\boldsymbol{y}) G(\boldsymbol{x}-\boldsymbol{y}) d\boldsymbol{y}.
\end{aligned} \tag{2.29}
$$

Note that, for the representation via the divergence operator to hold, we need to require that the convolutions $b_i * G$ exist in $\mathcal{D}'$; see [24]. A convenient sufficient condition for that may be $\boldsymbol{b}$ having compact support, which, as we have seen in section 2.2, does not present a significant restriction of generality from the standpoint of active control of sound. To make sure that the function $u(\boldsymbol{x})$ of (2.29) does solve the equation $\boldsymbol{L}u = b$, we apply the operator $\boldsymbol{L}$ of (1.1) to it:

$$
\begin{aligned}
\boldsymbol{L}u(\boldsymbol{x}) &= -\boldsymbol{L}\left[\sum_{i=1}^{n} b_i * \nabla_i G\right] = -\sum_{i=1}^{n} \boldsymbol{L}\left[b_i * \nabla_i G\right] \\
&= -\sum_{i=1}^{n} b_i * \boldsymbol{L}\nabla_i G = -\sum_{i=1}^{n} b_i * \nabla_i \boldsymbol{L}G = -\sum_{i=1}^{n} b_i * \nabla_i \delta = b(\boldsymbol{x}).
\end{aligned}
$$

Again, for the foregoing chain of equalities to hold, we need to require the existence of some convolutions in $\mathcal{D}'$, this time $b_i * \nabla_i G$, $i = 1, \ldots, n$. This is guaranteed by the same sufficient condition of $\mathrm{supp}\boldsymbol{b}$ being compact.

From the previous discussion we see that mathematically we can describe volumetric sources of time-harmonic sound only in terms of monopoles. In a real-life acoustic setting, however, both the actual monopole and the dipole sources may be present. It is instrumental to see how those sources that have different physical interpretation enter the right-hand side of the Helmholtz operator. We postpone the corresponding discussion till section 4.1, in which we provide the motivation for selecting a particular optimization criterion. In the meantime, let us emphasize that in the rest of the paper we are going to analyze only one type of the control sources, namely, the monopoles. This class includes all of the volumetric controls (2.1), i.e., monopoles distributed in space, and their limiting case given by the monopole layer on the surface $\Gamma$ (cf. formula (2.20)):

$$
g_{\mathrm{monopole}}^{(\mathrm{surf})} = -\left[\frac{\partial w}{\partial \boldsymbol{n}} - \frac{\partial u}{\partial \boldsymbol{n}}\right]_{\Gamma} \delta(\Gamma), \tag{2.30}
$$

where $w = w(\boldsymbol{x})$ in (2.30) solves the Dirichlet problem (2.23).[3] In other words, we have narrowed down the class of admissible controls by excluding the surface

[3] As has been mentioned (see section 4.1), volumetric monopoles considered in the mathematical perspective may include contributions from both actual physical monopoles and dipoles.

dipoles. Clearly, having only one and the same type of sources greatly facilitates their description and comparison using the same quantitative characteristics, e.g., acoustic strength (see [11] for the definition and section 4 for more detail). In particular, it allows us to formulate (see section 4.1) and solve (see sections 4.2 and 4.3) the optimization problem for the control sources with the overall absolute acoustic source strength being the cost function. Moreover, the solution of this optimization problem, i.e., the global minimum (more precisely, largest lower bound) in the class of all volumetric controls that guarantee the exact cancellation of noise, happens to be the uniquely defined single layer (2.30), (2.23) on the interface $\Gamma$. In this framework, surface dipoles naturally fall out of consideration.

There are, however, optimization criteria that employ physically meaningful quantities other than the total source strength, which naturally justify using combinations of both monopole and dipole control sources. These criteria would typically compare outputs of controls rather than the controls themselves. For example, in the forthcoming paper [8] we employ one such criterion, which is based on the power required by the control system. It turns out that the corresponding analysis necessarily involves interaction between the sources of sound and the surrounding acoustic field. Even though it may seem counterintuitive at a first glance, one can build a control system (a particular combination of monopoles and dipoles) that would require no power input for operation and would even produce a net power gain while providing exact noise cancellation. This, of course, comes at the expense of having the original sources of noise produce even more energy; see [8].

**3. Discrete control sources.** Similarly to the continuous constructions of the previous section, one can discretize the problem on the grid and obtain the control sources for the discrete formulation. From the standpoint of applications this is, of course, preferred, because any practical design of a noise control system can contain only a finite number of elements or devices (acoustic sensors and actuators) that will be associated with the grid nodes in the discrete case. Details regarding the discrete formulation of the noise control problem can be found in the monograph by Ryaben'kii [15, Part VIII], as well as in the papers [22, 23]; here we provide only a brief account of the corresponding work. The analysis hereafter will not be limited to any specific type of the grid. In particular, no adaptation or grid fitting to either the shape of the protected region $\Omega$ (i.e., interface $\Gamma$) or that of the external artificial boundary will generally be required. In some cases, though, it may simply be convenient and inexpensive to use a regular grid of an appropriate geometry. For example, as we discuss later, having a polar or spherical grid may greatly simplify setting the ABCs on the circle or sphere, respectively, of radius $R$ in the discrete framework.

**3.1. Grids and discretization.** Let us now introduce a finite-difference grid $\mathbb{N}$ that would span both $\Omega$ and $\Omega_1$. In the discrete formulation, the grid never stretches all the way to infinity; it is always truncated by the external artificial boundary, which implies that the discrete control sources that we obtain will always be compactly supported. Later in section 3.3, we will discuss how to set the appropriate ABCs for the discrete formulation. Now let $u^{(h)}$ be a representation of the acoustic field on the grid, and $\boldsymbol{L}^{(h)}$ be a finite-difference approximation of the differential operator $\boldsymbol{L}$ of (1.1). To accurately define the approximation, we will need to introduce another grid $\mathbb{M}$ along with the previously defined $\mathbb{N}$. On the grid $\mathbb{M}$, we will consider the residuals of the operator $\boldsymbol{L}^{(h)}$, and subsequently the right-hand sides to the corresponding inhomogeneous finite-difference equation. We will use the notations $n$ and $m$ for the individual nodes of the grids $\mathbb{N}$ and $\mathbb{M}$, respectively, and the notation $\mathbb{N}_m$ for the stencil of the discrete operator $\boldsymbol{L}^{(h)}$ centered at a given $m \in \mathbb{M}$, so that

$$\boldsymbol{L}^{(h)} u^{(h)}\big|_m = \sum_{n \in \mathbb{N}_m} a_{mn} u_n^{(h)}, \tag{3.1}$$

where $a_{nm}$ are the coefficients associated with particular nodes of the stencil. There are no limitations to the type of discrete operators that one may use. We only require that the difference operator $\boldsymbol{L}^{(h)}$ of (3.1) approximate the differential operator $\boldsymbol{L}$ of (1.1) with the accuracy sufficient for a particular application.

Next, we introduce the following subsets of the grids $\mathbb{M}$ and $\mathbb{N}$, which will allow us to accurately distinguish between the interior and exterior domains, interior and exterior sources, and interior and exterior solutions on the discrete level:

$$\begin{gathered} \mathbb{M}^+ = \mathbb{M} \cap \Omega, \quad \mathbb{M}^- = \mathbb{M} \backslash \mathbb{M}^+ = \mathbb{M} \cap \Omega_1, \\ \mathbb{N}^+ = \bigcup_{m \in \mathbb{M}^+}, \quad \mathbb{N}^- = \bigcup_{m \in \mathbb{M}^-} \mathbb{N}_m, \\ \gamma = \mathbb{N}^+ \cap \mathbb{N}^-, \quad \gamma^+ = \mathbb{N}^- \cap \Omega, \quad \gamma^- = \mathbb{N}^+ \cap \Omega_1. \end{gathered} \tag{3.2}$$

We emphasize that the grid $\mathbb{M}$ that pertains to the residuals of the finite-difference operator $\boldsymbol{L}^{(h)}$ is partitioned into $\mathbb{M}^+$ and $\mathbb{M}^-$ directly, i.e., following the geometry of $\Omega$ and $\Omega_1$. In contradistinction to that, the grid $\mathbb{N}$ is not partitioned directly; we rather consider the collection of all nodes of $\mathbb{N}$ swept by the stencil $\mathbb{N}_m$ when its center belongs to $\mathbb{M}^+$, and call this subgrid $\mathbb{N}^+$; see (3.2). Obviously, some of the nodes of $\mathbb{N}^+$ obtained by this approach happen to be outside $\Omega$, i.e., in $\Omega_1$, and these nodes are called $\gamma^-$. The sets $\mathbb{N}^-$ and $\gamma^+$ are defined similarly starting from $\mathbb{M}^-$. The key idea is that whereas the grids $\mathbb{M}^+$ and $\mathbb{M}^-$ do not overlap, the grids $\mathbb{N}^+$ and $\mathbb{N}^-$ do overlap, and their overlap is denoted $\gamma$; obviously, $\gamma = \gamma^+ \cup \gamma^-$. The subset of grid nodes $\gamma$ is called *the grid boundary*; it is a fringe of nodes that is located near the continuous boundary $\Gamma$ and in some sense straddles it. The specific structure of $\gamma$ obviously depends on the construction of the operator $\boldsymbol{L}^{(h)}$ of (3.1) and the stencil $\mathbb{N}_m$. For example, for the conventional second-order central-difference Laplacians on rectangular grids, $\gamma$ will be a two-layer fringe of grid nodes located near $\Gamma$, as shown schematically in Figure 3.1. Further specifics on the construction of grid boundaries can be found in the monograph [15].

**3.2. Discrete noise control problem and its general solution.** Having introduced the discretization (3.1) and grid subsets (3.2), we can formulate and solve the noise control problem on the grid. We will reproduce below the key results of [15, Part VIII]; see also [22, 23] for detail.

The discrete noise control problem is formulated similarly to the continuous one; see section 1. Let $f_m^{(h)+}$, $m \in \mathbb{M}^+$, and $f_m^{(h)-}$, $m \in \mathbb{M}^-$, be the interior and exterior discrete acoustic sources, respectively. Let $u_n^{(h)+}$, $n \in \mathbb{N}$, and $u_n^{(h)-}$, $n \in \mathbb{N}$, be the corresponding solutions, i.e., $\boldsymbol{L}^{(h)} u^{(h)+} = f^{(h)+}$ and $\boldsymbol{L}^{(h)} u^{(h)-} = f^{(h)-}$. Using the same terminology as before, we will call $u^{(h)+}$ the discrete sound and $u^{(h)-}$ the discrete noise. The overall discrete acoustic field $u^{(h)}$ is the sum of its sound and noise components, $u^{(h)} = u^{(h)+} + u^{(h)-}$ on $\mathbb{N}$, and obviously satisfies the equation $\boldsymbol{L}^{(h)} u^{(h)} = f^{(h)} \equiv f^{(h)+} + f^{(h)-}$. The goal is to obtain the discrete control sources $g^{(h)} = g_m^{(h)}$ so that the solution $\tilde{u}^{(h)}$ of the equation $\boldsymbol{L}^{(h)} \tilde{u}^{(h)} = f^{(h)+} + f^{(h)-} + g^{(h)}$ will be equal to only the sound component $u^{(h)+}$ on the subgrid $\mathbb{N}^+$.

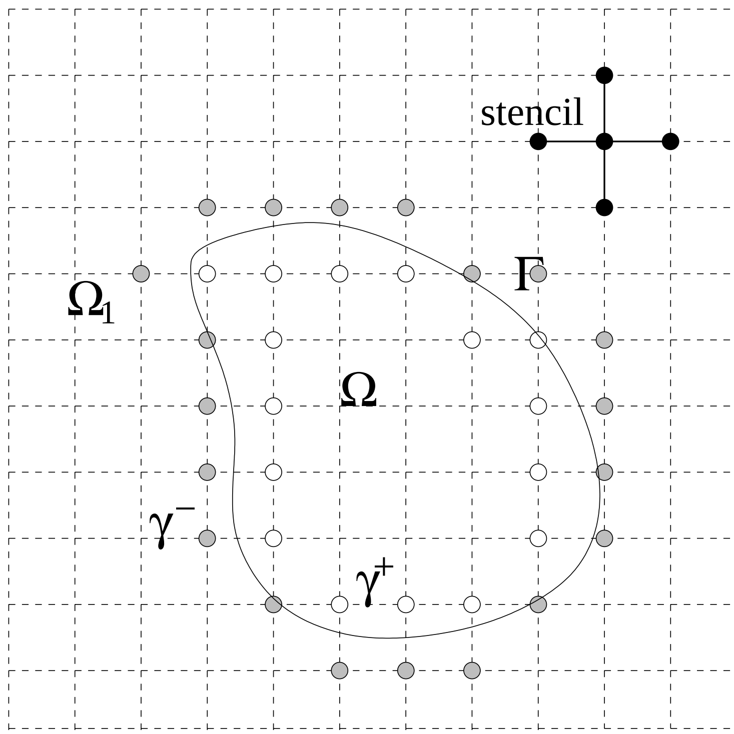


FIG. 3.1. *Schematic geometry of the domains, the stencil, and the grid boundary* $\gamma = \gamma^+ \cup \gamma^-$*: Hollow circles denote* $\gamma^+$*, filled circles denote* $\gamma^-$*.*

Let us now recall that, in the continuous case, the unique solvability of the governing differential equation (inhomogeneous Helmholtz' equation) was guaranteed by the Sommerfeld radiation conditions (1.2a) or (1.2b) at infinity. In the discrete case, we also need to guarantee the unique solvability of the foregoing finite-difference equations, but we obviously cannot directly set the boundary conditions at infinity. Therefore, the Sommerfeld radiation conditions have to be replaced by some other boundary conditions set at a finite location. To preserve the physics of the model that involves the propagation of waves toward infinity, one may choose to set the appropriate ABCs at the external artificial boundary that truncates our domain.[4] We emphasize that previously, i.e., in the continuous case, we have introduced and used the ABCs (see section 2.2) only for the purpose of obtaining compactly supported controls. Those ABCs were applied to the auxiliary function-parameter $w(\boldsymbol{x})$ (see (2.13) or (2.17)). In the discrete case, the ABCs should apply to the actual solutions $u^{(h)}$, $u^{(h)+}$, $u^{(h)-}$, and $\tilde{u}^{(h)}$, which represent the acoustic fields on the grid. For the purpose of constructing the controls, however, we will never need to implement the ABCs for the acoustic solutions on the grid explicitly. We will only need to know that these boundary conditions can be obtained (a variety of different approaches can be found, e.g., in [19]) and that they will guarantee the solvability of the difference equations involved.

[4]These ABCs would guarantee that the interior solution can be extended beyond the artificial boundary, so that the extension solves the Helmholtz equation and displays the correct far-field behavior.

There will, of course, be an explicit role for the ABCs in the discrete framework as well. We will employ these boundary conditions in the same capacity as we have used the original continuous ABCs (see section 2.2). Namely, when obtaining compactly supported controls, the ABCs will truncate the corresponding discrete function-parameter $w^{(h)}$. A specific approach to constructing the discrete ABCs that we use in this work is based on discretization of the continuous ABCs of section 2.2, and we discuss it in section 3.3. Altogether, both the discrete acoustic fields and the discrete-function parameter that is used for constricting the control sources (see formula (3.3) below) are going to satisfy the same ABCs. This is similar to the continuous case, when both the solution itself (i.e., acoustic field) and the function-parameter $w$ satisfied the same Sommerfeld radiation conditions at infinity.

The general solution for the discrete control sources $g^{(h)} = g_m^{(h)}$ that eliminate the unwanted noise $u^{(h)-}$ on $\mathbb{N}^+$ is given by the following formula (cf. formula (2.1)):

$$g_m^{(h)} = -\boldsymbol{L}^{(h)} w^{(h)}\big|_{m\in\mathbb{M}^-}, \tag{3.3}$$

where $w^{(h)} = w_n^{(h)}$, $n \in \mathbb{N}^-$, is a special auxiliary grid function-parameter that parameterizes the family of controls (3.3). The requirements that this function $w^{(h)}$ must satisfy are, again, rather "loose," and can be considered natural discrete counterparts of the corresponding requirements of the continuous function-parameter $w(\boldsymbol{x})$; see the discussion around formula (2.2) in section 2.1. Namely, at the grid boundary $\gamma$ the function $w^{(h)}$ has to coincide with the overall acoustic field $u^{(h)}$ to be controlled:

$$w_n^{(h)}\big|_{n\in\gamma} = u_n^{(h)}\big|_{n\in\gamma}. \tag{3.4}$$

We note that since, e.g., for the second-order discretizations the grid boundary $\gamma$ contains two layers of nodes, $\gamma^+$ and $\gamma^-$ (see Figure 3.1), then specifying the corresponding nodal values on $\gamma$ is in some sense equivalent to specifying the function and its normal derivative on $\Gamma$ in the continuous case; see (2.2). Of course, this is not a rigorous statement from the standpoint of approximation; we will address the approximation-related issues later on. We also note that when creating practical designs, the boundary data $u_n^{(h)}\big|_{n\in\gamma}$ shall be interpreted as measurable quantities that provide input for the control system. In other words, we can think of a microphone at every node of $\gamma$; these microphones measure the characteristics of the actual acoustic field and generate the input signal $u_n^{(h)}\big|_{n\in\gamma}$.

The other requirement of $w^{(h)}$, besides the interface boundary conditions (3.4), has already been mentioned. The function $w^{(h)}$ must satisfy the appropriate discrete ABCs at a finite external artificial boundary. The role of the discrete ABCs is the same as that of the continuous ABCs—to provide a replacement for the Sommerfeld radiation boundary conditions. This is done in the same approximate sense as the operator $\boldsymbol{L}^{(h)}$ approximates $\boldsymbol{L}$; see section 3.3. Other than the two aforementioned requirements, the function $w^{(h)}$ is arbitrary and, as such, parameterizes a substantial variety of discrete control sources; see (3.3). The latter will provide the search space for optimization in section 4.

The justification for formula (3.3) as the general solution for the discrete control sources is based on the theory of difference potentials; see [15]. In the framework of this theory one can show that the solution $v^{(h)} = v_n^{(h)}$ of the equation $\boldsymbol{L}^{(h)} v^{(h)} = g^{(h)}$ subject to the appropriate ABCs, where $g^{(h)}$ is defined according to (3.3) and (3.4), will be equal to exactly $-u^{(h)-}$ on the interior subgrid $\mathbb{N}^+$: $v_n^{(h)}\big|_{n\in\mathbb{N}^+} = -u^{(h)-}\big|_{n\in\mathbb{N}^+}$.

In other words, when the controls $g^{(h)}$ of (3.3) are added to the original source terms of the governing finite-difference equation, they annihilate the unwanted noise on the domain of interest in the discrete sense, i.e., on the grid. The aforementioned solution $v_n^{(h)}\big|_{n\in\mathbb{N}^+}$ is called the generalized difference potential with the density $-u_n^{(h)}\big|_{n\in\gamma}$ defined on the grid boundary $\gamma$. It is shown in the theory of difference potentials (see [15]) that the potential depends only on its density $-u_n^{(h)}|_{n\in\gamma}$ and not on the values of the function-parameter outside $\gamma$: $w_n^{(h)}|_{n\in\mathbb{N}^-\setminus\gamma}$. Consequently, all possible controls $g^{(h)}$ obtained according to (3.3), with different $w^{(h)}$'s subject only to (3.4) and the corresponding ABCs (see section 3.3), will produce identical output on $\mathbb{N}^+$ that will cancel out the unwanted noise $u_n^{(h)-}|_{n\in\mathbb{N}^+}$. This provides room for optimization of the discrete control sources; see section 4. It can also be shown that every discrete control source $g_m^{(h)}|_{m\in\mathbb{M}^-}$ that cancels out $u_n^{(h)-}|_{n\in\mathbb{N}^+}$ can be represented in the form (3.3) with some function $w^{(h)} = w_n^{(h)}$, $n \in \mathbb{N}^-$, that satisfies (3.4) and the external boundary conditions (ABCs). Similarly to the continuous case, this is done by explicitly constructing the appropriate $w^{(h)}$ for a given $g^{(h)}$ and $u_n^{(h)}|_{n\in\gamma}$; we refer the reader to [15, Part VIII] and [22, 23] for detail.

As has been mentioned, the cancellation of noise in the discrete framework is obtained on the grid $\mathbb{N}^+$. It is important to understand in what sense this discrete cancellation models the continuous cancellation described in section 2. This is basically the question of approximation of the continuous generalized potentials by the discrete ones. To that effect, the theory of difference potentials (see [15]) says that, under certain natural conditions, the difference potential $v^{(h)} = v_n^{(h)}$, $n \in \mathbb{N}^+$, i.e., the solution to $\boldsymbol{L}^{(h)}v^{(h)} = g^{(h)}$ with $g^{(h)}$ given by (3.3), approximates the continuous Calderon's potential $v = v(\boldsymbol{x})$, $\boldsymbol{x} \in \Omega$ (see (2.9)), i.e., the solution to $\boldsymbol{L}v = g$ with $g$ given by (2.1). The aforementioned natural conditions include first the consistency and stability of the finite-difference scheme for the Helmholtz equation. Consistency and stability will guarantee convergence as the grid size vanishes. In addition, the discrete boundary data $u_n^{(h)}|_{n\in\gamma}$ of (3.4) have to approximate the continuous boundary data $(u, \frac{\partial u}{\partial \boldsymbol{n}})|_\Gamma$ of (2.2) in the following sense. Once the continuous function $u$ and its first-order normal derivative $\frac{\partial u}{\partial \boldsymbol{n}}$ are known at the boundary $\Gamma$, normal derivatives of higher orders can be obtained via the differential equation itself, and the near-boundary values $u_n^{(h)}|_{n\in\gamma}$ can be calculated using Taylor's expansion; the order of accuracy of the latter calculation with respect to the grid size $h$ has to be at least as high as the order of accuracy of the interior scheme. In this case, the quality of approximation, i.e., the rate of convergence of the discrete potential to the continuous one with respect to $h$, will be the same as prescribed by the finite-difference scheme itself. For the second-order central-difference schemes discussed in sections 3.3 and 4, this rate is $O(h^2)$. In other words, when designing an active control system following the finite-difference approach, one can expect to have the actual noise cancellation in the same approximate sense as the solution of the finite-difference equation approximates the corresponding solution of the original differential equation. Note that in any particular practical setting we will need to require sufficient wave resolution on the grid, i.e., the waves of length $\lambda = 2\pi/k$, where $k$ is the wavenumber in (1.1), will have to be well resolved by the specific discretization.

**3.3. Specific discretization and discrete artificial boundary conditions.** As has been mentioned, one can use different approaches to construct discrete ABCs (see, e.g., [19]) that are needed to obtain compactly supported controls. The most

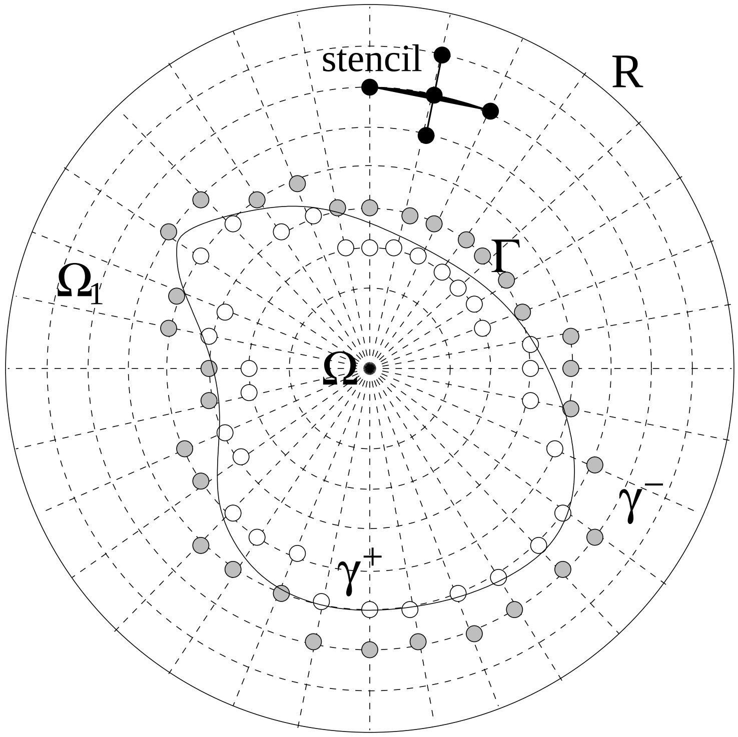


FIG. 3.2. *Schematic geometry of the domains, the stencil, and the grid boundary $\gamma = \gamma^+ \cup \gamma^-$ in polar coordinates: Hollow circles denote $\gamma^+$, filled circles denote $\gamma^-$.*

straightforward technique, which is adopted in the current study, although it is apparently not the most general one, is to directly approximate the continuous boundary conditions (2.13) or (2.17) with sufficient order of accuracy. For that, we will need a grid that would be fitted to the shape of the external artificial boundary, i.e., a polar or spherical grid. An example of the corresponding grid subsets $\gamma^+$ and $\gamma^-$ for polar coordinates is schematically shown in Figure 3.2.

In all numerical experiments that follow in section 4, we use a two-dimensional setup. Accordingly, we introduce a polar grid that has $J$ cells in the radial direction with the nodes $\rho_j = j\Delta\rho$, $j = 0, \dots, J$, so that $\rho_0 = 0$ and $\rho_J = R$, and $L$ cells in the circumferential direction with the nodes $\theta_s = s\Delta\theta$, $s = 0, \dots, L$, so that $\theta_0 = 0$ and $\theta_L = 2\pi$. For simplicity, it is convenient to assume that the grid sizes $\Delta\rho = R/J$ and $\Delta\theta = 2\pi/L$ are constant; in applications, the grid in the radial direction may be stretched; see section 4.2.

The Helmholtz equation is discretized on this grid with second-order accuracy by central differences:

$$\begin{aligned} \boldsymbol{L}^{(h)} w^{(h)}\big|_{s,j} \equiv {} & \frac{1}{\rho_j}\frac{1}{\Delta\rho}\left(\rho_{j+\frac{1}{2}}\frac{w^{(h)}_{s,j+1} - w^{(h)}_{s,j}}{\Delta\rho} - \rho_{j-\frac{1}{2}}\frac{w^{(h)}_{s,j} - w^{(h)}_{s,j-1}}{\Delta\rho}\right) \\ & + \frac{1}{\rho_j^2}\frac{w^{(h)}_{s+1,j} - 2w^{(h)}_{s,j} + w^{(h)}_{s-1,j}}{\Delta\theta^2} + k^2 w^{(h)}_{s,j} = 0. \end{aligned} \tag{3.5}$$

The left-hand side of (3.5) is a particular realization of the operator (3.1) that employs the five-node stencil shown in Figure 3.2. This operator will be used in section 4 for obtaining optimal discrete control sources.

To construct the finite-difference ABCs at $\rho = R$, we will also consider a semi-discrete form of the homogeneous equation in the far field:

$$\frac{1}{\rho}\frac{d}{d\rho}\left(\rho\frac{dw_s}{d\rho}\right) + \frac{1}{\rho^2}\frac{w_{s+1} - 2w_s + w_{s-1}}{\Delta\theta^2} + k^2 w_s = 0, \quad s = 0, \dots, L-1. \tag{3.6}$$

Introducing the direct and inverse discrete Fourier transforms, $l = -L/2+1, \dots, L/2$, $s = 0, \dots, L-1$,

$$\hat{w}_l = \frac{1}{L}\sum_{s=0}^{L-1} w_s e^{-ils\Delta\theta}, \qquad w_s = \sum_{l=-L/2+1}^{L/2} \hat{w}_l e^{ils\Delta\theta}, \tag{3.7}$$

we reduce (3.6) to the following system of ordinary differential equations with respect to $\hat{w}_l = \hat{w}_l(\rho)$:

$$\frac{1}{\rho}\frac{d}{d\rho}\left(\rho\frac{d\hat{w}_l}{d\rho}\right) - \frac{\alpha_l^2}{\rho^2}\hat{w}_l + k^2\hat{w}_l = 0, \quad \alpha_l^2 = \frac{4}{\Delta\theta^2}\sin^2\frac{l\Delta\theta}{2}, \quad \rho \geq R, \tag{3.8}$$

where again $l = -L/2+1, \dots, L/2$. Equations (3.8) are the same as (2.14), except that in the discrete case the range for $l$ is finite, and $l^2$ in (2.14) has been replaced by $\alpha_l^2$ in (3.8). Therefore, we can use the same boundary conditions (2.17) for $l = -L/2+1, \dots, L/2$,

$$\left.\frac{d}{d\rho}\hat{w}_l\right|_{\rho=R} = \hat{w}_l(R)\frac{\frac{d}{d\rho}H^{(2)}_{\alpha_l}(kR)}{H^{(2)}_{\alpha_l}(kR)}, \tag{3.9}$$

only with the Hankel functions of order $l$ replaced by the Hankel functions of the order $\alpha_l$. For implementation in the foregoing discrete framework, boundary conditions (3.9) for all $l = -L/2+1, \dots, L/2$ have to be approximated with second-order accuracy, which can be easily done as follows:

$$\frac{\hat{w}_{l,J} - \hat{w}_{l,J-1}}{\Delta\rho} - \beta_l\frac{\hat{w}_{l,J} + \hat{w}_{l,J-1}}{2} = 0, \qquad \beta_l = \frac{\frac{d}{d\rho}H^{(2)}_{\alpha_l}(kR)}{H^{(2)}_{\alpha_l}(kR)}. \tag{3.10}$$

Finally, relations in (3.10) for all $l = -L/2+1, \dots, L/2$ can be rewritten in the matrix form:

$$\boldsymbol{w}_{\cdot,J} = \boldsymbol{F}^{-1}\text{diag}\left\{-\left(\frac{1}{\Delta\rho} + \beta_l\right)\left(\frac{1}{\Delta\rho} - \beta_l\right)^{-1}\right\}\boldsymbol{F}\,\boldsymbol{w}_{\cdot,J-1} \equiv \boldsymbol{T}\,\boldsymbol{w}_{\cdot,J-1}, \tag{3.11}$$

where $\boldsymbol{F}$ and $\boldsymbol{F}^{-1}$ are matrices of the direct and inverse discrete Fourier transforms of (3.7), and $\boldsymbol{w}_{\cdot,J}$ and $\boldsymbol{w}_{\cdot,J-1}$ are $L$-dimensional vectors of components $w^{(h)}_{s,J}$ and $w^{(h)}_{s,J-1}$, respectively, $s = 0, 1, \dots, L-1$.

In the three-dimensional case, instead of the discrete Fourier transforms (3.7) one can use expansions with respect to the so-called finite-difference spherical functions (see [15, Part IV, Chapter 4]) that form a full orthogonal system of eigenvectors for the spherical part of the discrete Laplacian. Other than that, the construction of the discrete three-dimensional ABCs will be similar to the foregoing two-dimensional construction. We do not expand on it here because we do not conduct three-dimensional computations in this paper. Let us also mention that for small $l$ the difference between $l^2$ and the corresponding $\alpha_l^2$ (see (3.8)) will obviously be small as well. Therefore, for smooth functions $w$, for which the short-wave part of the spectrum (large $l$'s) is insignificant, one may not even have to replace $l$ in (2.17) by $\alpha_l$ in (3.9). We have observed this type of behavior in the previous paper [14], in which we studied similar questions for the Poisson equation.

**3.4. Types of discrete control sources.** Similarly to the continuous case (see section 2.3) let us now identify some particular types of discrete control sources. First, we define another subset of the grid $\mathbb{M}$ (more precisely, of $\mathbb{M}^-$):

$$\mathbb{M}^-_{\text{int}} = \left\{ m \in \mathbb{M}^- \middle| \mathbb{N}_m \cap \gamma^+ = \emptyset \right\}.$$

Basically, $\mathbb{M}^-_{\text{int}}$ is the interior subset of $\mathbb{M}^-$ such that, when the center of the stencil sweeps this subset, the stencil itself does not touch $\gamma^+$; see Figures 3.1 and 3.2. In other words, we can say that $\mathbb{M}^-_{\text{int}}$ is a subset of $\mathbb{M}^-$ such that

$$\bigcup_{m \in \mathbb{M}^-_{\text{int}}} \mathbb{N}_m = \mathbb{N}^- \backslash \gamma^+.$$

Having defined this new subset $\mathbb{M}^-_{\text{int}}$, we now introduce the auxiliary function $w^{(h)} = w_n^{(h)}$, $n \in \mathbb{N}^-$, for (3.3) as follows:

$$w_n^{(h)}\big|_{n\in\gamma^+} = u_n^{(h)}\big|_{n\in\gamma^+}, \tag{3.12a}$$

and

$$\begin{aligned} &w_n^{(h)}\big|_{n\in\gamma^-} = u_n^{(h)}\big|_{n\in\gamma^-}, \\ &\boldsymbol{L}^{(h)} w^{(h)} = 0 \quad \text{on} \quad \mathbb{M}^-_{\text{int}}. \end{aligned} \tag{3.12b}$$

As before, we also assume that $w^{(h)}$ satisfies the appropriate discrete ABCs; see, e.g., (3.11). Definition (3.12a) means that on the interior part of the grid boundary $\gamma^+$ we simply set $w^{(h)}$ equal to the given $u^{(h)}$: $w_n^{(h)}|_{n\in\gamma^+} = u_n^{(h)}|_{n\in\gamma^+}$. Definition (3.12b) is actually a discrete exterior boundary-value problem of the Dirichlet type. Indeed, everywhere on and "outside" the exterior part of the grid boundary $\gamma^-$, i.e., on $\mathbb{N}^-\backslash\gamma^+$, the grid function $w^{(h)}$ is obtained as a solution of the homogeneous equation $\boldsymbol{L}^{(h)} w^{(h)} = 0$ (enforced at the nodes $\mathbb{M}^-_{\text{int}}$) supplemented by the boundary data on $\gamma^-$: $w_n^{(h)}\big|_{n\in\gamma^-} = u_n^{(h)}\big|_{n\in\gamma^-}$, which is specified for the unknown function $w^{(h)}$ itself. Note, relation (3.12a) and the first relation (3.12b) together are obviously equivalent to (3.4). Therefore, the function $w^{(h)}$ defined via (3.12a), (3.12b) falls into the general class of $w^{(h)}$'s used for obtaining the discrete control sources; see section 3.2.

Problem (3.12b) can clearly be considered a finite-difference counterpart to the continuous Dirichlet problem (2.23). Therefore, it is natural to call the control sources $g^{(h)} \equiv g^{(\text{h,surf})}_{\text{monopole}}$ obtained by formulae (3.3), (3.12a), (3.12b) *the discrete surface monopoles.* Indeed, because of the definition of $w^{(h)}$ given by (3.12a) and (3.12b), these $g^{(\text{h,surf})}_{\text{monopole}}$ may, generally speaking, differ from zero only on the grid set $\mathbb{M}^-\backslash\mathbb{M}^-_{\text{int}}$, which is a single "curvilinear" layer of nodes of grid $\mathbb{M}$ that follows the geometry of Γ. Accordingly, the output of these controls can be called the discrete single-layer potential; it was first introduced and analyzed in our recent paper [20]. Let us emphasize that unlike the continuous surface monopoles (2.30), which belong to a different class of functions rather than the volumetric sources (2.1) and (2.2) (singular $\delta$-type distributions vs. regular locally integrable functions), the foregoing discrete surface monopoles belong to the same original class of discrete control sources (3.3) and (3.4). They can be considered as the ultimate reduction of the volumetric discrete controls (3.3) and (3.4) to the surface. In section 4, the discrete surface monopoles will play a fundamental role for the analysis of the optimization problems.

Besides the discrete surface monopoles and the corresponding single-layer potential, one can also define the discrete surface dipoles and, accordingly, the double-layer potential; see [20]. Grid dipoles are introduced for the pairs of neighboring nodes so that the nodes in the pair are assigned values equal in magnitude and opposite in sign. The control sources in the form of discrete surface dipoles can be obtained by solving a special Neumann-type discrete exterior boundary-value problem for the auxiliary function $w^{(h)}$, which would be analogous to the continuous problem (2.24). The construction of surface dipoles, however, is somewhat more elaborate than the foregoing definition of surface monopoles. And because in this paper we basically focus on the monopole-type sources only, we are not going to further elaborate here on the issue of discrete surface dipoles, but will rather refer the reader to our paper [20] for detail.

**4. Optimization of control sources.** Once the general solution for controls is available, in either continuous (2.1) or discrete (3.3) formulation, the next step is to decide what particular element of this large family of functions will be optimal for a specific setting. There is a multitude of possible criteria for optimality that one can use; we discuss some of them in the forthcoming papers [8, 9]. We should also emphasize that in many practical problems the cancellation of noise is only approximate, and, as such, the key criterion for optimization (or sometimes, the key constraint) is the quality of this cancellation, i.e., the extent of noise reduction. In contradistinction to that, in this paper we are considering ideal, or exact, cancellation; i.e., every particular control field from either the continuous (2.1) or discrete (3.3) family completely eliminates the unwanted noise on the domain of interest. Consequently, the criteria for optimality of the controls that we can employ will not include the level of the residual noise as a part of the corresponding function of merit, and should rather depend only on the control sources themselves. We realize, of course, that at a later stage of the work we will also need to look into the issues of approximate, rather than exact, noise cancellation, for the reason of further reducing the costs. In this case, optimal solutions found in the framework of the exact cancellation are likely to provide good initial guesses for subsequent optimization in the approximate framework. Moreover, it will probably be possible to use some results from the approximation theory to deal with the issues of approximate noise cancellation once we have solutions for the exact cancellation. We expect that this approach will be much faster than any algorithm of combinatorial type. A similar reduction in computational complexity of optimization was outlined in our earlier work [6] on the optimal distributed control of the exterior Stokes flow.

**4.1. Optimization in the sense of $L_1$.** To derive a meaningful criterion for optimization of the control sources, let us first discuss the physical meaning of the quantities involved in the formulation of the problem. The most natural way to interpret the field variable $u = u(\boldsymbol{x})$ (as well as its discrete counterpart $u_n^{(h)}$) is to call it acoustic pressure. Indeed, acoustic pressure is the quantity which is directly measured by the sensing devices (microphones), and as such can be immediately supplied as the required boundary input data for the control system; see formulae (2.2) and (3.4). We now recall that in the current paper we only analyze a single-frequency formulation of the noise control problem. To better understand the nature of the source terms in the Helmholtz equation that governs the time-harmonic pressure $u = u(\boldsymbol{x})$, we will now examine the original unsteady acoustic formulation. Let $p = p(\boldsymbol{x}, t)$ be the actual acoustic pressure, and $\boldsymbol{v} = \boldsymbol{v}(\boldsymbol{x}, t)$ be the velocity of fluid particles. Then, the acoustics system can be written as

$$\begin{aligned} \frac{\partial \rho(\boldsymbol{x}, t)}{\partial t} + \rho_0 \operatorname{div} \boldsymbol{v}(\boldsymbol{x}, t) &= \rho_0 q_{\text{vol}}(\boldsymbol{x}, t), \\ \rho_0 \frac{\partial \boldsymbol{v}(\boldsymbol{x}, t)}{\partial t} + \operatorname{grad} p(\boldsymbol{x}, t) &= \boldsymbol{b}_{\text{vol}}(\boldsymbol{x}, t), \end{aligned} \tag{4.1}$$

where $\rho_0$ is the density of the ambient fluid. The quantity $q_{\text{vol}}$ on the right-hand side of the continuity equation in (4.1) is known as the volume velocity per unit volume; see, e.g., [10, 11]. It is defined through the actual volume velocity $q = \int_S v_n d\sigma$, which is the integral of the normal component of the fluid particles' velocity $v_n$ evaluated over a closed surface $S$; then $q_{\text{vol}} = \lim_{V \to +0} \frac{1}{V} \int_S v_n d\sigma$, where $V$ is the volume enclosed by $S$. The physical meaning of the sources $\rho_0 q_{\text{vol}}$ is that they excite the medium by altering the balance of mass in the system, i.e., by injecting/draining certain amounts of fluid. Clearly, in the time-harmonic context the process of injecting/draining the fluid has to be periodic.

Similarly, the quantity $\boldsymbol{b}_{\text{vol}}$ on the right-hand side of the second equation of (4.1) shall be interpreted as the force per unit volume. Obviously, it excites the medium by altering the balance of momentum in the system; and again, in the time-harmonic context the net force applied to the fluid particles has to be periodic. Altogether, we see that two types of sources can be introduced in unsteady acoustics that are distinctly different from the standpoint of physics. Next, we will see that they can be interpreted as monopoles and dipoles, respectively, as introduced in section 2.3.

We apply the adiabatic law $p = c^2 \rho$, where $c$ is the speed of sound (constant), differentiate the first equation of (4.1) with respect to time, take the divergence of the second equation of (4.1), and substitute into the first one, which yields the inhomogeneous wave equation for the acoustic pressure:

$$-\frac{1}{c^2} \frac{\partial^2 p(\boldsymbol{x}, t)}{\partial t^2} + \Delta p(\boldsymbol{x}, t) = \operatorname{div} \boldsymbol{b}_{\text{vol}}(\boldsymbol{x}, t) - \rho_0 \frac{\partial q_{\text{vol}}(\boldsymbol{x}, t)}{\partial t}. \tag{4.2}$$

The second term on the right-hand side of (4.2) is the volume acceleration per unit volume multiplied by the ambient fluid density. The Helmholtz equation for the time-harmonic pressure is obtained by Fourier transforming (4.2) in time, which formally amounts to replacing the temporal derivatives $\frac{\partial}{\partial t}(\,\cdot\,)$ by $-i\omega(\,\cdot\,)$. For simplicity we will keep all the notations the same except that the time-harmonic problem quantities will depend only on $\boldsymbol{x}$ and not on $t$, and we will also use the previous notation $u(\boldsymbol{x})$ for the Fourier transformed pressure $p(\boldsymbol{x}, t)$:

$$\Delta u(\boldsymbol{x}) + k^2 u(\boldsymbol{x}) = \operatorname{div} \boldsymbol{b}_{\text{vol}}(\boldsymbol{x}) + i\omega \rho_0 q_{\text{vol}}(\boldsymbol{x}). \tag{4.3}$$

The wavenumber $k$ in the Helmholtz equation (4.3) is given by $k = \omega / c$, where $\omega$ is the frequency of the original temporal oscillations.

Clearly, (4.3) is basically the same as (1.1), except that in (4.3) we provide a detailed description of the source terms based on their physical origin. Namely, we see that the scalar sources $q_{\text{vol}}$ that alter the acoustic balance of mass (see (4.1)) enter the right-hand side of the Helmholtz equation directly (up to a multiplicative constant), whereas the sources $\boldsymbol{b}_{\text{vol}}$ that alter the acoustic balance of momentum (see (4.1)) enter the right-hand side of the Helmholtz equation through a divergence operator. Therefore, the analysis of section 2.3 allows us to interpret $q_{\text{vol}}(\boldsymbol{x})$ as genuine volumetric monopoles and $\boldsymbol{b}_{\text{vol}}(\boldsymbol{x})$ as volumetric dipoles that are rewritten as equivalent monopoles $\text{div}\boldsymbol{b}_{\text{vol}}(\boldsymbol{x})$ for mathematical convenience.

The latter operation, namely, recasting the physical dipoles into the monopole form, allows us to qualitatively study and optimize both types of sources in a uniform manner. In acoustics (see [10]), the overall right-hand side $f(\boldsymbol{x}) = \text{div}\boldsymbol{b}_{\text{vol}}(\boldsymbol{x}) + i\omega\rho_0 q_{\text{vol}}(\boldsymbol{x})$ of (4.3) is often referred to as *the acoustic source density.* As we have seen, the meaning of this right-hand side is excitation per unit volume. Accordingly, the integral of this quantity over a given region, $\int_V f d\boldsymbol{x}$, is referred to as *the acoustic source strength* that pertains to the sources in this region, and the integral of its magnitude, $\int_V |f| d\boldsymbol{x}$, is known as *the absolute acoustic source strength.* If the actual sources involved in the consideration were only monopoles, then the acoustic source strength would obviously coincide with the overall volume velocity $q$, and the acoustic source density would coincide with the volume velocity per unit volume $q_{\text{vol}}$.

For distributed sources, the acoustic source density is assumed to be finite; in particular, for distributed genuine monopoles the associated volume velocity per unit volume is assumed to be finite. In the case of an isolated point monopole, i.e., a $\delta$-type source (see section 2.3), which can be represented as a vanishingly small oscillating sphere of radius $\epsilon$ with surface velocity $v_\epsilon$, the volume velocity can be introduced as $q = \lim_{\epsilon\to+0} v_\epsilon 4\pi\epsilon^2$. When the strength $q$ of this isolated monopole is finite, the associated source density is formally infinite (which is natural to expect for a $\delta$-type source). In the case of a continuous distribution of sources, the relationship between the source density and source strength is standard (like that between the mass density and total mass, electric charge density and total charge, etc.) and basically says that the integral of the source density over a given region is equal to the overall source strength associated with this region. In other words, the acoustic source density is equal to the acoustic source strength per unit volume.

Obviously, the physical meaning of the quantity $g = g(\boldsymbol{x})$ of (2.1) that describes the control sources is the same as that of the original right-hand side $f = f(\boldsymbol{x})$ of (1.1) that we have recently specified according to (4.3). Namely, $g(\boldsymbol{x})$ shall be interpreted as *the acoustic source strength per unit volume* (up to a multiplicative constant) of the control sources. It is important to mention that as we are studying the time-harmonic traveling waves, all the quantities involved in the formulation of the problem are complex-valued. This is essential, as otherwise it would not have been possible to account for the key phenomenon of the variation of phase between different spatial locations.

Having identified the physical meaning of the variables involved in the noise control model that we have adopted, we would argue in the current paper for selecting the optimal control sources based on minimization of their *overall absolute acoustic source strength.* Mathematically, this translates into the minimization of the $L_1$ norm of the control sources:

$$\|g\|_1 \equiv \int_{\text{supp}\, g} |g(\boldsymbol{x})| d\boldsymbol{x} \longrightarrow \min, \tag{4.4}$$

where the search space for minimization in (4.4) includes all the appropriate auxiliary functions $w(\boldsymbol{x})$, by means of which the controls $g(\boldsymbol{x})$ are defined (see formulae (2.1), (2.2), and the discussion in the beginning of section 2.1). The advantage of using this criterion for optimization is that it has a clear physical interpretation, and the quantities involved, the volume velocity as well as the force applied to fluid particles, actually characterize the corresponding engineering devices (actuators in the active noise control system). For comparison, we note that the criterion based on the $L_2$ norm,

$$\|g\|_2 \equiv \sqrt{\int_{\operatorname{supp} g} |g(\boldsymbol{x})|^2 d\boldsymbol{x}} \longrightarrow \min,$$

does not have a similar clear physical interpretation, although as indicated below (see also our forthcoming paper [9]), the corresponding numerical optimization problem is much easier to solve. Another advantage of using the $L_1$ norm, or in other words, the overall absolute acoustic source strength, as the cost function for optimization (minimization) is that it characterizes only the control sources themselves. This is a convenient distinction compared, e.g., to the power-based criteria, which, as has been mentioned, would always involve interaction between the sources and the field they operate in. This interaction is often referred to as the "load" on the sources by the field (see [11]), and may lead to certain types of degeneration when solving the optimization problem; see [8].

In the discrete framework, the $L_1$ minimization problem that corresponds to (4.4) is formulated as follows:

$$\|g^{(h)}\|_1 \equiv \sum_{m \in \mathbb{M}^- \cap \{\rho < R\}} V_m |g^{(h)}_m| \longrightarrow \min, \tag{4.5}$$

where $V_m$ accounts for the volume in three dimensions or area in two dimensions of a particular grid cell, and again, the search space includes all the appropriate auxiliary grid functions $w^{(h)}$ through which $g^{(h)}$ is defined; see formula (3.3). The function $w^{(h)}$ is supposed to satisfy boundary conditions (3.4) on the interface, and the selected ABCs at the external artificial boundary; for the two-dimensional examples analyzed in the following section 4.2 the latter will be boundary conditions (3.11).

Let us now return to the definition (3.3) of the discrete control sources $g^{(h)}$ and adopt the polar framework of section 3.3. The finite-difference operator $\boldsymbol{L}^{(h)}$ can obviously be interpreted as a matrix with $N$ columns and $M$ rows, where $N$ is the number of nodes $n \equiv (s, j)$ of the grid $\mathbb{N}^-$ such that the corresponding radial coordinate $\rho_j \leq R$, i.e., $j \leq J$, and $M$ is the number of nodes $m \equiv (s, j)$ of the grid $\mathbb{M}^-$ such that the corresponding radial coordinate $\rho_j < R$, i.e., $j \leq J - 1$. Denote by $\boldsymbol{w}$ the vector of $N$ components $w^{(h)}_n \equiv w^{(h)}_{s,j}$ such that $n \in \mathbb{N}^-$ and $j \leq J$. The components of $\boldsymbol{w}$ can obviously be arranged in a particular way so that this vector can then be decomposed into four subvectors:

$$\boldsymbol{w} = [\boldsymbol{w}_\gamma, \boldsymbol{w}_0, \boldsymbol{w}_{\cdot,J-1}, \boldsymbol{w}_{\cdot,J}]^T, \tag{4.6}$$

where $\boldsymbol{w}_\gamma$ contains all those and only those $w^{(h)}_n$ for which $n \in \gamma$, $\boldsymbol{w}_{\cdot,J}$, and $\boldsymbol{w}_{\cdot,J-1}$ correspond to the outermost and second-to-last circles of the polar grid, respectively, as in formula (3.11), and $\boldsymbol{w}_0$ contains all the remaining components of $\boldsymbol{w}$. In accordance with (4.6), the matrix $\boldsymbol{L}^{(h)}$ can be decomposed into four submatrices:

$$\boldsymbol{L}^{(h)} = [\boldsymbol{A}, \boldsymbol{B}, \boldsymbol{C}, \boldsymbol{D}], \tag{4.7}$$

where the number of rows in all four is the same and equal to $M$, $\boldsymbol{A}$ has as many columns as there are nodes in $\gamma$ (we denote this number $|\gamma|$), $\boldsymbol{C}$ and $\boldsymbol{D}$ each have $L$ columns (see section 3.3), and the number of columns in $\boldsymbol{B}$ is obviously $N-|\gamma|-2L$.

Using representations (4.6) and (4.7), one can rewrite the optimization problem (4.5) as follows:

$$\|\boldsymbol{V}(\boldsymbol{A}\boldsymbol{w}_\gamma + \boldsymbol{B}\boldsymbol{w}_0 + \boldsymbol{C}\boldsymbol{w}_{\cdot,J-1} + \boldsymbol{D}\boldsymbol{w}_{\cdot,J})\|_1 \longrightarrow \min, \tag{4.8}$$

where the norm in (4.8) is a conventional $L_1$ norm on complex $M$-dimensional vectors, and $\boldsymbol{V}$ is an $M \times M$ diagonal matrix with the entries given by the corresponding cell areas $V_m$. Next, we recall that the search space for optimization (4.5) is composed of all the appropriate grid functions $w^{(h)}$, which means that the vector $\boldsymbol{w}$ in the optimization formulation (4.8) is, in fact, subject to a number of equality-type constraints that come from the interface conditions (3.4) and ABCs (3.11). More precisely, the first subvector $\boldsymbol{w}_\gamma$ in (4.6) is known and fixed because of (3.4), and we can rewrite (3.4) as $\boldsymbol{w}_\gamma = \boldsymbol{u}_\gamma$, where $\boldsymbol{u}_\gamma$ is given. The last subvector $\boldsymbol{w}_{\cdot,J}$ in (4.6) is a function of $\boldsymbol{w}_{\cdot,J-1}$ according to (3.11). Therefore, we can conclude that only $\boldsymbol{w}_0$ and $\boldsymbol{w}_{\cdot,J-1}$ contain free variables that provide the search space for optimization, and as such rewrite (4.8) as

$$\min_{\boldsymbol{w}_0,\boldsymbol{w}_{\cdot,J-1}} \|\boldsymbol{V}(\boldsymbol{B}\boldsymbol{w}_0 + (\boldsymbol{C}+\boldsymbol{D}\boldsymbol{T})\boldsymbol{w}_{\cdot,J-1} + \boldsymbol{A}\boldsymbol{w}_\gamma)\|_1 \equiv \min_{\boldsymbol{z}} \|\boldsymbol{E}\boldsymbol{z}-\boldsymbol{f}\|_1, \tag{4.9}$$

where $\boldsymbol{E} = \boldsymbol{V}[\boldsymbol{B}, \boldsymbol{C}+\boldsymbol{D}\boldsymbol{T}]$ is an $M \times (N-|\gamma|-L)$ given matrix, $\boldsymbol{z} = [\boldsymbol{w}_0, \boldsymbol{w}_{\cdot,J-1}]^T$ is an $(N-|\gamma|-L)$-dimensional vector of unknowns, and $\boldsymbol{f} = -\boldsymbol{V}\boldsymbol{A}\boldsymbol{w}_\gamma$ is an $M$-dimensional known vector of the right-hand side. Minimization problem (4.9) is, in fact, a problem of finding a weak solution in the sense of $L_1$ of an overdetermined complex linear system $\boldsymbol{E}\boldsymbol{z} = \boldsymbol{f}$.

Let us first note that the most conventional weak formulation for an overdetermined system $\boldsymbol{E}\boldsymbol{z} = \boldsymbol{f}$ would be that in the sense of $L_2$, rather than (4.9). The $L_2$ minimization problem $\|\boldsymbol{E}\boldsymbol{z}-\boldsymbol{f}\|_2 \longrightarrow \min$ has proven easy to solve numerically even for rather complex geometries. It does not require the Moore–Penrose-type arguments and can be conveniently solved by a standard QR algorithm; we report the corresponding results in our forthcoming paper [9]. As has been mentioned, though, this formulation lacks a convincing physical interpretation and therefore, hereafter we concentrate on solving the $L_1$ optimization problem (4.9).

By introducing $M$ additional real variables $t_i \in \mathbb{R}$, $i = 1, \ldots, M$, one can reduce problem (4.9) to the following optimization problem with equality-type constraints,

$$\begin{gathered} \min \sum_i t_i, \\ \left|\sum_j e_{ij} z_j - f_i\right| - t_i = 0, \quad i = 1, \ldots, M, \end{gathered} \tag{4.10}$$

which is equivalent to the problem with inequality-type constraints:

$$\begin{gathered} \min \sum_i t_i, \\ \left|\sum_j e_{ij} z_j - f_i\right| - t_i \le 0, \quad i = 1, \ldots, M. \end{gathered} \tag{4.11}$$

If all the quantities involved in the formulation (4.9) were real, then problem (4.11) would, in turn, be equivalent to the linear programming problem (see [21, Chapter 12, section 4]):

$$\begin{aligned} &\min \sum_i t_i, \\ &-t_i \le \sum_j e_{ij} z_j - f_i \le t_i, \quad i = 1, \dots, M, \end{aligned} \tag{4.12}$$

which nowadays can be solved efficiently even for large dimensions. However, complex entries in $\boldsymbol{E}$, $\boldsymbol{z}$, and $\boldsymbol{f}$ (see (4.9)) are essential in order to account for traveling waves, so we will actually need to solve *a nonlinear problem* (4.11) rather than a linear problem (4.12).

The most obvious disadvantage of optimizing in the sense of $L_1$ is that the foregoing problem (4.11) appears very difficult to solve numerically. Besides being nonlinear, the constraints are obviously nonsmooth. Moreover, strictly speaking, those constraints are not convex either. Indeed, for every $i = 1, \dots, M$, the inequality $|\sum_j e_{ij} z_j - f_i| - t_i \le 0$ defines a cone in the space of variables $t_i$, $\Re(\sum_j e_{ij} z_j - f_i)$, and $\Im(\sum_j e_{ij} z_j - f_i)$. As we are only considering the upper half of the cone, this set is geometrically convex. However, algebraically the function $|\sum_j e_{ij} z_j - f_i|^2 - t_i^2$ of variables $z_j$, $t_i$ obviously cannot be convex. And the algebraic convexity (i.e., positive semidefiniteness of the Hessian) is exactly what distinguishes between the convex and nonconvex programming problems, with the latter being substantially more difficult to treat in a numerical setting; see [21, Chapter 24]. Of course, problem (4.11) can be reformulated so that the constraints will become truly convex:

$$\begin{aligned} &\min \sum_i \sqrt{t_i}, \\ &\left| \sum_j e_{ij} z_j - f_i \right|^2 - t_i \le 0, \quad i = 1, \dots, M. \end{aligned} \tag{4.13}$$

However, in the formulation (4.13) the most "harmless" cost function that one can think of, i.e., the linear function $\sum_i t_i$, has been replaced by the function $\sum_i \sqrt{t_i}$ that has singular derivatives at the optimum. Experimentally, we have observed that this presents even more severe problems for a numerical optimizer.

Altogether, the combination of nonlinearity, nonsmoothness, and only "marginal" convexity (optimization over cones) makes problem (4.11) a serious challenge even for the most sophisticated state-of-the-art approaches to numerical optimization—the approaches that are typically based on interior point methods [12, 21]. The difficulties are further exacerbated by the large dimension of the grid on which the problem is formulated. Even for the aforementioned state-of-the art methods the maximum number of constraints that they can handle is typically on the order of hundreds. And in problem (4.11), the number of constraints is the same as the number of grid nodes $M$. As such, one can easily encounter an orders of magnitude difference between the number of constraints that the numerical optimizer will handle and the number of grid nodes that will make the formulation of an active noise control problem practically interesting. This is especially true for three-dimensional problems.

In spite of all difficulties, we have still managed to obtain numerical solutions in two space dimensions for some simple test cases. All numerical experiments that we have conducted indicate a very consistent behavior of the $L_1$-optimal solution for control sources; it happens to be the discrete layer of monopoles on the surface $g^{(\mathrm{h,\,surf})}_{\mathrm{monopole}}$ described in section 3.4. Recall, this solution is obtained by applying formula (3.3) to the auxiliary function $w^{(h)}$ defined by (3.12a), (3.12b). In the following section 4.2, we report the corresponding computational results, and in the subsequent section 4.3, we provide a general proof of the global $L_1$-optimality of this surface monopole solution in the case of one space dimension. Overall, the combination of the two-dimensional numerical evidence and the one-dimensional general proof prompts us to put forward a conjecture (see section 5) that the foregoing uniquely defined layer of surface monopoles always provides the control sources with minimal total absolute strength. This conjecture implies that the difficult procedure of numerical optimization in the sense of $L_1$ *can actually be bypassed* when building the $L_1$-optimal control sources; the latter can be obtained by simply solving the boundary-value problem (3.12b), which is an easy task. In other words, assuming that our arguments toward global minimality of surface monopoles are sufficiently convincing (see sections 4.2 and 4.3), we can claim that finding the $L_1$-optimal controls will now take only a most straightforward computation, apparently even easier than optimization in the sense of $L_2$; see [9]. Of course, comparison of the different optimization strategies in the framework of an approximate, rather than exact, noise cancellation will require a through future study.

**4.2. Numerical solution of the $L_1$-optimization problem.** For our numerical simulations, we have considered the simplest possible two-dimensional geometric setup, with the protected domain $\Omega$ in the form of a disk of radius $r = 1$ centered at the origin. The external artificial boundary was a circle of radius $R > r$, as in section 3.3. As such, the resulting discrete control sources were concentrated within the annular region $r \le \rho \le R$.

In contradistinction to section 3.3, here we have used a polar grid, which was stretched in the radial direction. This allowed us to keep the cell aspect ratio constant. The grid is first built in the coordinates $(\ln\rho, \theta)$; it has equal square cells $\frac{2\pi}{L} \times \frac{2\pi}{L}$ and is constructed on the rectangle $[-\frac{2\pi}{L}, \ln R] \times [0, 2\pi]$. Then, the conformal mapping $e^{\ln\rho + i\theta}$ maps it onto a polar grid with uniform angular spacing $\theta_s = s\Delta\theta$, where $\Delta\theta = \frac{2\pi}{L}$ and $s = 0, \dots, L$, so that $\theta_0 = 0$ and $\theta_L = 2\pi$, and nonuniform radial spacing $\rho_j = \exp\left(\frac{2\pi}{L} \cdot j\right)$, $j = -1, 0, \dots, J$, so that $\rho_{-1} = \exp\left(-\frac{2\pi}{L}\right)$, $\rho_0 = 1 = r$, and $\rho_J = R$. It is convenient to define the grid sizes in the radial direction as $\Delta\rho_j \equiv \rho_j - \rho_{j-1} = \exp\left(\frac{2\pi}{L} \cdot j\right) - \exp\left(\frac{2\pi}{L} \cdot (j-1)\right)$, $j = 0, \dots, J$. The Helmholtz operator can be easily approximated on this new nonuniform grid with the second order of accuracy using the same five-node stencil as shown in Figure 3.2. This involves little change compared to the approximation (3.5), which works for uniform grids, and we refer the reader to our paper [14] for detail. The discrete ABCs (3.10) or (3.11) do not change, except that $\Delta\rho_J$ needs to be substituted instead of $\Delta\rho$.

As we are building our control sources outside of the protected region $\Omega = \{(\rho,\theta) \,|\, \rho < r = 1\}$, i.e., on $\Omega_1 = \mathbb{R}^2 \backslash \Omega$, we do not need to be concerned with the structure of the grid inside $\Omega$. For our constructions, we will only need to use one grid circle inside $\Omega$. This will be the innermost circle $j = -1$. The second to innermost circle $j = 0$ already represents the interface $\Gamma = \partial\Omega = \{(\rho,\theta) \,|\, \rho = r = 1\}$.

Adopting the definition (3.2) of the grid subsets introduced in section 3.1, we obtain

(4.14)
$$\begin{gathered}\mathbb{M}^+ = \{(\rho_j, \theta_s) \,|\, j = -1\}, \quad \mathbb{M}^- = \{(\rho_j, \theta_s) \,|\, 0 \le j \le J-1\}, \\ \mathbb{N}^+ = \{(\rho_j, \theta_s) \,|\, j = -1, 0\}, \quad \mathbb{N}^- = \{(\rho_j, \theta_s) \,|\, -1 \le j \le J\}, \\ \gamma = \{(\rho_j, \theta_s) \,|\, j = -1, 0\}, \quad \gamma^+ = \{(\rho_j, \theta_s) \,|\, j = -1\}, \quad \gamma^- = \{(\rho_j, \theta_s) \,|\, j = 0\}.\end{gathered}$$

For all definitions in (4.14), we assume $s = 0, \dots, L-1$.

In the computational experiments, we have used grids with four times the number of cells in the circumferential direction compared to the radial direction. Specific grid dimensions were: $L = 32$ and $L = 48$, and accordingly, $J = 7$ and $J = 11$. (Note, as $j = -1, 0, \dots, J$, the number of cells in the radial direction is $J+1$.) The wavenumber $k$ in the Helmholtz equation (1.1) was chosen as $k = 0.5$. The excitation, i.e., the acoustic field $u^{(h)}$ that drives the control system, was taken in the analytic form of a shifted fundamental solution (see formula (2.3a)), as if it were generated by the point source $\delta(\boldsymbol{x} - \boldsymbol{x}_1)$, where $\boldsymbol{x}_1 = (\rho\cos\theta, \rho\sin\theta) = (5, 0)$. We reemphasize that our approach does not require an explicit knowledge of the exterior sources of noise. We only need this function $u^{(h)}$ as a sample field to be used as given data in formula (3.4).

We have also considered another case: $L = 48$, $J = 9$; for this case, we have selected $k = 0.9$. The excitation was produced by two point sources, $\delta(\boldsymbol{x} - \boldsymbol{x}_1) + \delta(\boldsymbol{x} - \boldsymbol{x}_2)$, where $\boldsymbol{x}_1 = (5, 0)$ and $\boldsymbol{x}_2 = (1, 2)$. Note, as for the wavenumber we have $k = \omega/c$, where $\omega$ is the temporal frequency and $c$ is the speed of sound (see section 4.1). We also obtain the following relation between the wavelength $\lambda$ and the wavenumber: $\lambda = 2\pi/k$. This means that in both cases, $k = 0.5$ and $k = 0.9$, we consider long waves relative to the diameter of the protected region $\Omega$, which has been found advantageous from the standpoint of convergence of the numerical optimization algorithm.

The matrices and vectors involved in the formulation of the optimization problem (4.9) were constructed in accordance with the chosen geometric setup. Namely, the dimension of $\boldsymbol{L}^{(h)}$ (see (4.7)) was $M \times N \equiv (L \cdot J) \times (L \cdot (J+2))$; the dimension of $\boldsymbol{A}$, which corresponds to the variables on $\gamma$, was $M \times 2 \cdot L \equiv (L \cdot J) \times 2 \cdot L$; the dimension of $\boldsymbol{B}$ was $M \times (N - 4L) \equiv (L \cdot J) \times (L \cdot (J-2))$; and the dimension of either $\boldsymbol{C}$ or $\boldsymbol{D}$ was $M \times L \equiv (L \cdot J) \times L$.

We have tried several numerical approaches for solving the corresponding minimization problems (4.11), starting with the algorithms available as a part of the standard optimization toolbox in MATLAB. However, our best numerical results were obtained with the software package SeDuMi by J. F. Sturm.[5] This is a numerical algorithm for optimization over cones [17]; it employs the ideas of interior point methods and the self-dual embedding technique of [25]; see also [13]. The algorithm allows for complex-valued entries, which is very important in our framework, and also for quasi-convex quadratic and positive semidefinite constraints. Of course, all the cases that we have been able to compute using SeDuMi (see above) can still be treated only as simple model examples on the scale of potential applications for noise control (see section 4.1). However, the optimal solutions that we have obtained all demonstrate a very coherent behavior that we discuss below. On Figures 4.1(a), 4.2(a), and 4.3(a) we plot magnitudes of the $L_1$ optimal solutions computed with SeDuMi [17]. Let us also note that SeDuMi is, in fact, a rather general procedure, and one may expect

[5] http://fewcal.kub.nl/sturm/software/sedumi.html

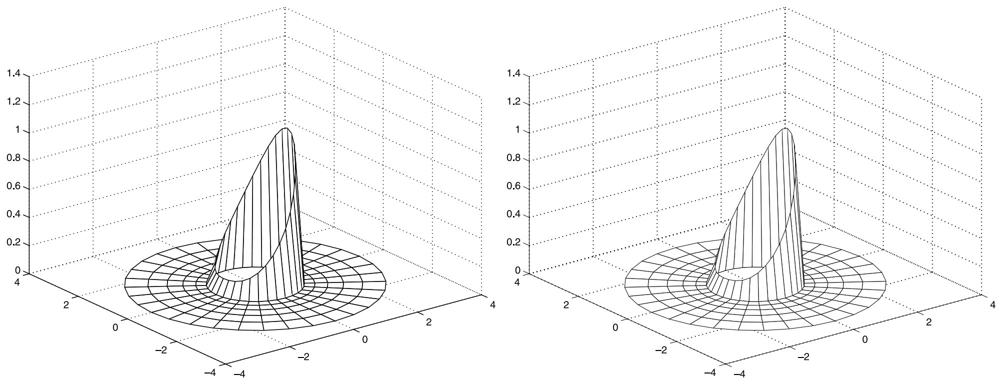


(a) $L_1$ optimal solution (b) Surface monopoles $g^{(\mathrm{h,surf})}_{\mathrm{monopole}}$

FIG. 4.1. *Control sources for* $L = 32$, $J = 7$, $k = 0.5$, *excitation* $\delta(\boldsymbol{x} - \boldsymbol{x}_1)$, $\boldsymbol{x}_1 = (5, 0)$.

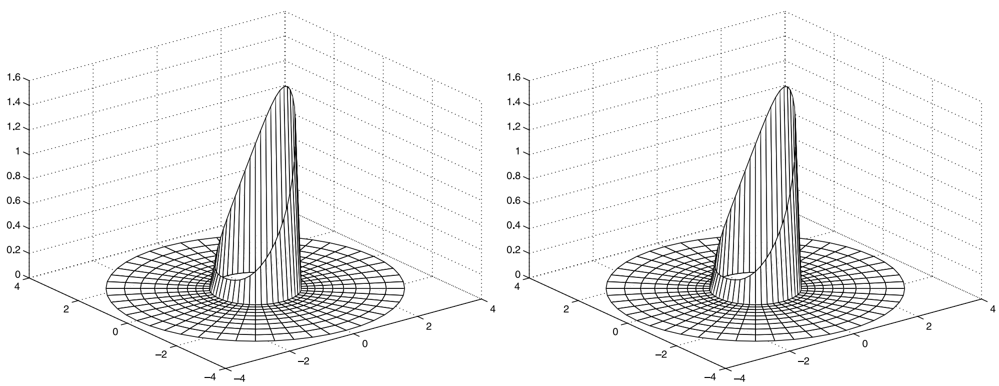


(a) $L_1$ optimal solution (b) Surface monopoles $g^{(\mathrm{h,surf})}_{\mathrm{monopole}}$

FIG. 4.2. *Control sources for* $L = 48$, $J = 11$, $k = 0.5$, *excitation* $\delta(\boldsymbol{x} - \boldsymbol{x}_1)$, $\boldsymbol{x}_1 = (5, 0)$.

better numerical performance from more focused algorithms, such as the one proposed by Andersen et al. in [1]. In the future, we may try the algorithm of [1] for solving the foregoing $L_1$ minimization problem.

Apparently, the most obvious observation that one can make by looking at Figures 4.1(a), 4.2(a), and 4.3(a) is that in all cases the optimal solution (i.e., the $L_1$ minimum) is concentrated on a single circumferential layer of grid nodes. This is the second to innermost circle of the grid $\mathbb{N}^-$ (see (4.14)), i.e., the grid line $j = 0$. It corresponds to the outer portion of the grid boundary $\gamma^-$ (see (4.14)), and, in the continuous case, to the interface $\Gamma$ itself, $\Gamma = \partial\Omega = \{(\rho, \theta) \,|\, \rho = r = 1\}$. In other words, the $L_1$-optimal solutions for control sources that we have computed can all be interpreted as layers of monopole sources on the perimeter of the protected region $\Omega$. This clearly calls for comparing these optimal solutions with the densities of discrete

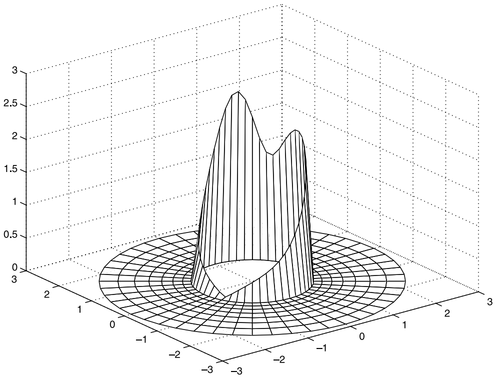

(a) $L_1$ optimal solution

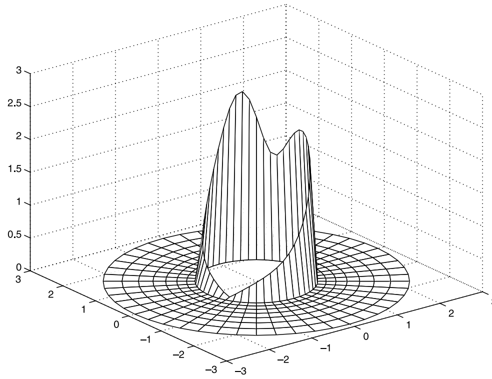

(b) Surface monopoles $g^{(\text{h,surf})}_{\text{monopole}}$

FIG. 4.3. *Control sources for $L = 48$, $J = 9$, $k = 0.9$, excitation $\delta(\boldsymbol{x} - \boldsymbol{x}_1) + \delta(\boldsymbol{x} - \boldsymbol{x}_2)$, $\boldsymbol{x}_1 = (5, 0)$, $x_2 = (1, 2)$.*

single-layer potentials introduced in section 3.4.

To conform the general definitions of section 3.4 to the specific geometric setup analyzed here, we need to construct on $\mathbb{N}^-\backslash\gamma^+$ the solution $w^{(h)}$ of the discrete exterior Dirichlet problem (3.12b) for the case when $\gamma^-$ is the grid circle $j = 0$. (In this case, $\mathbb{M}^-_{\text{int}}$ corresponds to $j > 0$.) Then, the operator $\boldsymbol{L}^{(h)}$ of (3.5) needs to be applied to the overall resulting function $w^{(h)}$, including its definition (3.12a) on the inner part $\gamma^+$ of the grid boundary: $w^{(h)}_n|_{n\in\gamma^+} = u^{(h)}_n|_{n\in\gamma^+}$. Since we know ahead of time that the resulting controls will differ from zero only on $\gamma^-$ (which is an equivalent of $\mathbb{M}^-\backslash\mathbb{M}^-_{\text{int}}$ in this case), we need not consider $w^{(h)}$ anywhere beyond $j = 1$. Consequently, for the purpose of constructing surface monopoles, we may simply set $J = 1$ and consider $w^{(h)}$ on three grid circles only: $j = -1$, $j = 0 \equiv J - 1$, and $j = 1 \equiv J$. In so doing, we obviously have to specify the ABCs (3.11) right on the interface; in other words, the input for the ABCs will be on $\gamma^-$, i.e., at $j = 0$, and the output will be on the outermost circle $j = J = 1$. Clearly, specifying the ABCs on $\gamma^-$ allows us to reconstruct $w^{(h)}_{s,j}$ for $j = J$ directly by formula (3.11), i.e., without actually solving the aforementioned exterior Dirichlet problem. And once we know $w^{(h)}$ for $j = -1$, 0, and 1, we can easily obtain the discrete surface monopole controls on $\gamma^-$, i.e., for $j = 0$. As in section 3.4, we will denote these control sources $g^{(\text{h,surf})}_{\text{monopole}}$.

In Figures 4.1(b), 4.2(b), and 4.3(b), we plot magnitudes of the discrete surface controls $g^{(\text{h,surf})}_{\text{monopole}}$ for the exact same cases, for which we have explicitly computed the $L_1$ minimal solutions using SeDuMi. Visually comparing Figures 4.1(a), 4.2(a), and 4.3(a) with respective Figures 4.1(b), 4.2(b), and 4.3(b), we conclude that there is virtually no difference between them. In other words, the $L_1$-optimal solutions coincide with the surface monopole control sources $g^{(\text{h,surf})}_{\text{monopole}}$. To further corroborate this conclusion, we evaluate the $L_1$ norm of the difference on the grid $\mathbb{M}^-$ between each $L_1$-optimal solution and the corresponding surface monopole layer $g^{(\text{h,surf})}_{\text{monopole}}$, assuming that $g^{(\text{h,surf})}_{\text{monopole}} = 0$ everywhere except on $\gamma^-$. The results are presented in Table 4.1.

The data in Table 4.1, which take into account both magnitude and phase, do

Table 4.1
*Comparison of the computed $L_1$-optimal solutions with surface monopoles.*

| Case | $\min_{w^{(h)}} \|g^{(h)}\|_{1,\mathbb{M}^-}$ | $\|g^{(\text{h,surf})}_{\text{monopole}}\|_{1,\mathbb{M}^-}$ | $\|g^{(h)}_{\min} - g^{(\text{h,surf})}_{\text{monopole}}\|_{1,\mathbb{M}^-}$ | Relative diff. |
|---|---|---|---|---|
| Figure 4.1 | 0.5764 | 0.5761 | 0.0067 | 0.0117 |
| Figure 4.2 | 0.5769 | 0.5761 | 0.0036 | 0.0063 |
| Figure 4.3 | 0.9760 | 0.9750 | 0.0083 | 0.0085 |

corroborate that the respective solutions are close to one another. Moreover, by comparing the second and third rows in Table 4.1, we can apparently observe the phenomenon of grid convergence. Indeed, the case of Figure 4.2 is computed on a grid which is 1.5 times finer in each direction than the grid of Figure 4.1. For a second-order scheme, we can consequently expect a drop in the error by a factor of $\sim 2.25$, which we indeed see in Table 4.1 for both the absolute and relative difference between the $L_1$ minimum $g^{(h)}_{\min}$ and surface monopoles $g^{(\text{h,surf})}_{\text{monopole}}$. Even though the solutions that we are computing are obviously not smooth, and thus the grid convergence may be difficult to justify analytically, the foregoing experimental observation certainly makes our point about the coincidence of $g^{(h)}_{\min}$ and $g^{(\text{h,surf})}_{\text{monopole}}$ even more convincing.

Summarizing the foregoing numerical results, we can see that in all the cases analyzed the minimum for the $L_1$ norms of the control sources $g^{(h)}$ on $\mathbb{M}^-$ (see (4.5)) is actually given by the $L_1$ norm of $g^{(\text{h,surf})}_{\text{monopole}}$:

$$\min_{w^{(h)}} \left\|g^{(h)}\right\|_{1,\mathbb{M}^-} = \left\|g^{(\text{h,surf})}_{\text{monopole}}\right\|_{1,\mathbb{M}^-}.$$

The right-hand side of the previous equality can be recast into a more natural form by noticing that surface controls $g^{(\text{h,surf})}_{\text{monopole}}$ are defined only on $\gamma^-$. Then we can replace the $L_1$ norm over the two-dimensional grid domain $\mathbb{M}^-$ by the $L_1$ norm over the "one-dimensional" grid subset $\gamma^-$. This will bring about a factor of $\Delta\rho_1$ because obviously the cell areas $V_m$ (see (4.5)) that correspond to nodes $j = 0$ are all equal and proportional to $\Delta\rho_1$. As such, we obtain

$$\min_{w^{(h)}} \left\|g^{(h)}\right\|_{1,\mathbb{M}^-} = \left\|g^{(\text{h,surf})}_{\text{monopole}}\right\|_{1,\gamma^-} \Delta\rho_1. \tag{4.15}$$

Equality (4.15) basically conjectures *global minimality of the surface monopole solution for active controls in the sense of $L_1$*.

As of yet, of course, we can only claim that equality (4.15) holds because it has been corroborated by a particular collection of numerical experiments that we have conducted. However, motivated by the consistency of our experimental observations that all suggest (4.15) (see Figures 4.1, 4.2, and 4.3 and Table 4.1), we have been able to prove a general result on the global $L_1$-optimality of the surface monopole solution for controls in both continuous and discrete formulation in the one-dimensional case. As has already been mentioned, we interpret the combination of the foregoing numerical results and the forthcoming analytic one-dimensional proof as an indication that surface monopoles may provide a universal global optimum in the sense of $L_1$. This, in particular, means that no numerical optimization will be needed for constructing the $L_1$-optimal control sources; they can simply be obtained by solving the boundary-value problem (3.12b) for the generating function $w^{(h)}$.

**4.3. One-dimensional proof of global $L_1$-optimality.** It will be convenient to consider simultaneously both the continuous and discrete formulations of the one-dimensional noise control problem. Let's denote the independent variable $x \in \mathbb{R}$ and introduce the one-dimensional Helmholtz equation for the field variable $u = u(x)$ (cf. (1.1)):

$$\boldsymbol{L}u \equiv \frac{d^2u}{dx^2} + k^2u = f(x). \tag{4.16}$$

Then we introduce a uniform grid $x_n = n \cdot h$, $n = 0, \pm 1, \pm 2, \dots,$ of variable $x$, and approximate (4.16) with the second-order central-difference scheme

$$\boldsymbol{L}^{(h)}u^{(h)} = \frac{u_{n+1}^{(h)} - 2u_n^{(h)} + u_{n-1}^{(h)}}{h^2} + k^2u_n^{(h)} = f_n^{(h)}. \tag{4.17}$$

Note that here we are using the same subscript "$n$" for both the discrete unknown function $u^{(h)}$ and the discrete right-hand side $f^{(h)}$, because for the particular scheme (4.17) they are defined on the same grid. We will still need to distinguish, however, between the grids $\mathbb{M}$ and $\mathbb{N}$ when constructing the necessary grid subsets.

Let us assume that our protected region $\Omega$ corresponds to $x < 0$ and accordingly, the complementary region $\Omega_1$ corresponds to $x \geq 0$. Then, the continuous control sources will be given by (cf. formula (2.1))

$$g(x) = -\frac{d^2w}{dx^2} - k^2w\bigg|_{x\geq 0}, \tag{4.18}$$

where the auxiliary function $w(x)$, $x \geq 0$, is supposed to satisfy the interface conditions (cf. formula (2.2))

$$w(0) = u(0), \qquad \frac{dw}{dx}\bigg|_{x=0} = \frac{du}{dx}\bigg|_{x=0} \tag{4.19}$$

and the appropriate ABC, i.e., the radiation boundary condition, as $x \longrightarrow +\infty$. The quantities $u(0)$ and $\frac{du}{dx}\big|_{x=0}$ in (4.19) are assumed to be given.

Next, applying the definitions of section 3.1 to a particular stencil given by (4.17), we will have $\mathbb{M}^+ = \{m \,|\, m \equiv n = -1, -2, \dots\}$, $\mathbb{M}^- = \{m \,|\, m \equiv n = 0, 1, 2, \dots\}$, $\mathbb{N}^+ = \{n \,|\, n = 0, -1, -2, \dots\}$, $\mathbb{N}^- = \{n \,|\, n = -1, 0, 1, 2, \dots\}$, and $\gamma = \{n \,|\, n = -1, 0\}$. Accordingly, the discrete one-dimensional control sources will be given by (cf. formula (3.3))

$$g_n^{(h)} = -\frac{w_{n+1}^{(h)} - 2w_n^{(h)} + w_{n-1}^{(h)}}{h^2} - k^2w_n^{(h)}\bigg|_{n\geq 0}, \tag{4.20}$$

where the auxiliary grid function $w_n^{(h)}$ is supposed to satisfy the interface conditions on $\gamma = \{n \,|\, n = -1, 0\}$ (cf. formula (3.4))

$$w_{-1}^{(h)} = u_{-1}^{(h)}, \qquad w_0^{(h)} = u_0^{(h)}, \tag{4.21}$$

and the appropriate ABC at infinity, or in other words, for large $n$'s. Again, the quantities $u_{-1}^{(h)}$ and $u_0^{(h)}$ in (4.21) are considered as given.

To obtain the continuous ABC, we assume that the auxiliary function $w(x)$ satisfies the homogeneous version of (4.16): $\boldsymbol{L}w = 0$ for $x \geq X > 0$. This equation has two linearly independent solutions: $e^{-ikx}$ is a right-traveling wave, and $e^{ikx}$ is a left-traveling wave. In the one-dimensional framework, we obviously need to treat the right-traveling wave as outgoing for the artificial outer boundary $x = X$. Therefore, employing the same mode selection principle as in section 2.2, we arrive at the following ABC (cf. formulae (2.13) and (2.17)):

$$\left.\frac{dw}{dx}\right|_{x=X} = -ikw(X), \tag{4.22}$$

which guarantees that only one of the two aforementioned linearly independent modes, namely $e^{-ikx}$, will remain in the composition of $w(x)$ for $x \geq X$. Note that boundary condition (4.22) can, in fact, be interpreted as the Sommerfeld radiation condition. In the one-dimensional case, it can be specified at a finite location, in contradistinction to the multidimensional case when these boundary conditions can only be specified at infinity; see formulae (1.2a), (1.2b). Altogether, the continuous auxiliary function $w = w(x)$ that defines the control sources $g(x)$ by formula (4.18) is specified on the interval $[0, X]$ and satisfies boundary conditions (4.19) and (4.22).

To obtain the discrete one-dimensional ABC, we will not approximate (4.22) with finite differences, as we did in section 3.3 for the polar case, when it was basically the only option. We will rather use a genuine finite-difference approach, which has shown efficient in many cases (see the review [19]), and which was studied in our recent paper [4] for a more complex formulation that involves a high-order approximation to the Helmholtz equation. Let's assume that the auxiliary grid function $w^{(h)}$ satisfies the homogeneous version of (4.17): $\left.\boldsymbol{L}^{(h)}w^{(h)}\right|_n = 0$ for $n \geq N > 0$ (one may think that $X = (N-1)\cdot h$). This homogeneous finite-difference equation has two linearly independent solutions: $q^n$ and $q^{-n}$, where $q$ and $q^{-1}$ are roots of the corresponding algebraic characteristic equation

$$q^2 - (2 - k^2h^2)q + 1 = 0. \tag{4.23}$$

These roots are given by the formulae:

$$q = 1 - \frac{1}{2}k^2h^2 - ikh\sqrt{1 - \frac{1}{4}k^2h^2}, \qquad q^{-1} = 1 - \frac{1}{2}k^2h^2 + ikh\sqrt{1 - \frac{1}{4}k^2h^2}. \tag{4.24}$$

It is easy to see from (4.24) that for small $h$ the discrete wave $q^n$ approximates the continuous right-traveling wave $e^{-ikx}$, and the discrete wave $q^{-n}$ approximates the continuous left-traveling wave $e^{ikx}$. Therefore, the solution $q^n$ shall be interpreted as a discrete outgoing wave, and $q^{-n}$ shall be interpreted as a discrete incoming wave, for the external artificial boundary $n = N$. To guarantee the radiation of waves, we need to select $q^n$ and prohibit $q^{-n}$, or in other words, require that $w_n^{(h)} = c \cdot q^n$ for $n \geq N$, where $c = \text{const}$. Accordingly, we arrive at the following discrete ABC:

$$w_N^{(h)} = q \cdot w_{N-1}^{(h)}, \tag{4.25}$$

which guarantees that only one of the two aforementioned linearly independent solutions, namely $q^n$, will remain in the composition of $w_n^{(h)}$ for $n \geq N$. Altogether, the auxiliary grid function $w^{(h)} = w_n^{(h)}$ that defines the control sources $g^{(h)}$ by formula (4.20) is specified on the grid subset $\{n \,|\, n = -1, 0, 1, \dots, N\}$ and satisfies boundary conditions (4.21) and (4.25).

From now on, we will be considering only the situation with no interior sources. In other words, the only field present in the model *before control* will be the incoming field with respect to the protected region $\Omega = \{x \in \mathbb{R} \,|\, x < 0\}$. In the continuous case it can be expressed as $u(x) \equiv u^-(x) = Ae^{ikx}$, and in the discrete case as $u_n^{(h)} \equiv u_n^{(h)-} = Aq^{-n}$, where $A = \text{const}$. This restriction, in fact, presents no loss of generality. Indeed, if we had both components, $u(x) = u^-(x) + u^+(x) = Ae^{ikx} + Be^{-ikx}$, and had chosen $w(x)$ according to (4.19) and (4.22), then we could have replaced this

$w(x)$ by $\tilde{w}(x) = w(x) - Be^{-ikx} \equiv w(x) - u^+(x)$. The function $\tilde{w}(x)$ would satisfy the new interface conditions $\tilde{w}(0) = u^-(0)$, $\frac{d\tilde{w}}{dx}\big|_{x=0} = \frac{du^-}{dx}\big|_{x=0}$ instead of (4.19), and the same original ABC (4.22). Most important, the control sources generated by this new auxiliary function according to (4.18) will be the exact same control sources as those generated by $w(x)$: $\boldsymbol{L}w = \boldsymbol{L}[\tilde{w} + Be^{-ikx}] = \boldsymbol{L}\tilde{w}$, $x \geq 0$. Similarly in the discrete case, if we had $u_n^{(h)} = u_n^{(h)-} + u_n^{(h)+} = Aq^{-n} + Bq^n$, then the auxiliary functions $w_n^{(h)}$ and $\tilde{w}_n^{(h)} = w_n^{(h)} - Bq^n \equiv w_n^{(h)} - u_n^{(h)+}$ would generate the exact same discrete control sources according to (4.20). Of course, the foregoing argument is in complete agreement with the general discussion of section 2 on insensitivity of the control sources to the interior sound.

In the continuous one-dimensional case, the interface between the protected region $\Omega = \{x \in \mathbb{R} \,|\, x < 0\}$ and its complement $\Omega_1 = \{x \in \mathbb{R} \,|\, x \geq 0\}$ is obviously one point, $x = 0$. To construct the corresponding "surface" monopole controls, we consider a special form of the auxiliary function $w(x)$. Namely, if the original field to be controlled is the left-traveling wave that propagates into $\Omega$, $u(x) = u^-(x) = Ae^{ikx}$, $x < 0$, then we take $w(x)$ in the form of the right-traveling wave: $w(x) = Ae^{-ikx}$, $x \geq 0$. Obviously, this function $w(x)$ solves the homogeneous equation on $\Omega_1$, $\boldsymbol{L}w = 0$, $x \geq 0$, and satisfies the ABC (4.18). It also satisfies the Dirichlet boundary condition at the interface $x = 0$: $w(0) = u(0)$. Altogether, we see that $w(x)$ selected this way solves the one-dimensional counterpart of the exterior Dirichlet problem (2.23) that we used in section 2.3 to obtain the control sources in the form of surface monopoles. According to the analysis of section 2.3, surface monopoles are obtained by applying the operator $-\boldsymbol{L}$ to the function $v$ of (2.21), which has discontinuous first derivative across the interface. In the specific one-dimensional case that we are studying here, this function is given by

$$v(x) = \begin{cases} Ae^{ikx} & \text{for} \quad x < 0, \\ Ae^{-ikx} & \text{for} \quad x \geq 0. \end{cases} \tag{4.26}$$

Applying the operator $-\boldsymbol{L}$ (see (4.16)) to the function $v(x)$ of (4.26) in the sense of distributions (see [24]), we obtain the following "surface" (in fact, point) monopole control source (cf. formula (2.30)):

$$g_{\text{monopole}}^{(\text{surf})} = 2Aik\delta(x). \tag{4.27}$$

To obtain the discrete "surface" monopoles in the one-dimensional case, we need to consider $u_n^{(h)} = Aq^{-n}$ for $n \leq 0$, and $w_n^{(h)} = Aq^n$ for $n \geq 0$; we also set $w_{-1}^{(h)} = u_{-1}^{(h)}$. The aforementioned $w_n^{(h)}$ solves the discrete homogeneous equation $\boldsymbol{L}^{(h)}w^{(h)} = 0$ for $n > 0$, satisfies the discrete ABC (4.25), and the interface conditions $w_\gamma^{(h)} = u_\gamma^{(h)}$, or equivalently (4.21). In other words, the selected $w^{(h)}$ solves the one-dimensional version of the exterior Dirichlet-type problem (3.12b), (3.12a) that we used in section 3.4 to derive surface monopole controls in the discrete framework. Applying the operator $-\boldsymbol{L}^{(h)}$ (see (4.17)) to the foregoing function $w^{(h)}$, we obtain the discrete surface control source

$$g_{\text{monopole}}^{(h,\,\text{surf})} = \begin{cases} -A\left(2\frac{q-1}{h^2} + k^2\right) & \text{for} \quad n = 0, \\ 0 & \text{for} \quad n > 0. \end{cases} \tag{4.28}$$

We are now prepared to formulate our central result on the global $L_1$-optimality of surface monopoles in the one-dimensional discrete framework. For any function $w^{(h)} = w_n^{(h)}$ that satisfies the ABC (4.25) and the interface conditions (4.21), where $u_n^{(h)} = Aq^{-n}$, $n \leq 0$, the $L_1$ norm of the corresponding control sources (4.20) will always be greater than or equal to the magnitude of the surface monopole (4.28) times the grid size $h$: $\|g^{(h)}\|_1 \geq |g^{(h,\,\mathrm{surf})}_{\mathrm{monopole}}|h$. In the case $w^{(h)}_n = Aq^n$ the equality is achieved, and thus $\min_{w^{(h)}} \|g^{(h)}\|_1 = |g^{(h,\,\mathrm{surf})}_{\mathrm{monopole}}|h$. In other words, the following theorem holds.

THEOREM 4.1. *Let a complex-valued function $w^{(h)} = w^{(h)}_n$ be defined on the grid $n = -1, 0, 1, \dots, N$, where $N > 0$ can be arbitrary. Let $w^{(h)}_0 = A$, where $A \in \mathbb{C}$ is a given constant, and $w^{(h)}_{-1} = qw^{(h)}_0$ and $w^{(h)}_N = qw^{(h)}_{N-1}$, where $q$ is defined by formula* (4.24). *Then,*

$$\min_{w^{(h)}_n} \sum_{n=0}^{N-1} \left| \frac{w^{(h)}_{n+1} - 2w^{(h)}_n + w^{(h)}_{n-1}}{h^2} + k^2 w^{(h)}_n \right| = |A| \left| 2\frac{q-1}{h^2} + k^2 \right|. \tag{4.29}$$

*Proof.* Let us introduce new quantities $p_0,\ p_1, \dots, p_{N-2}$ so that $w^{(h)}_1 = p_0 w^{(h)}_0$, $w^{(h)}_2 = p_1 w^{(h)}_1, \dots, w^{(h)}_{N-1} = p_{N-2} w^{(h)}_{N-2}$. Then the sum on the left-hand side of (4.29) can be recast in the following form (taking into account that $w^{(h)}_{-1} = qw^{(h)}_0$ and $w^{(h)}_N = qw^{(h)}_{N-1}$):

$$\begin{aligned}
&\sum_{n=0}^{N-1} \left| \frac{w^{(h)}_{n+1} - 2w^{(h)}_n + w^{(h)}_{n-1}}{h^2} + k^2 w^{(h)}_n \right| \\
&\quad = |A| \left| \frac{p_0 + q - 2}{h^2} + k^2 \right| + |A| \left| \frac{p_0 p_1 - 2p_0 + 1}{h^2} + k^2 p_0 \right| \\
&\quad + |A||p_0| \left| \frac{p_1 p_2 - 2p_1 + 1}{h^2} + k^2 p_1 \right| + |A||p_0||p_1| \left| \frac{p_2 p_3 - 2p_2 + 1}{h^2} + k^2 p_2 \right| + \cdots \\
&\quad + |A||p_0||p_1| \cdots |p_{N-3}| \left| \frac{p_{N-2} q - 2p_{N-2} + 1}{h^2} + k^2 p_{N-2} \right|.
\end{aligned}$$

Next, we introduce new notations: $p_0 = q + z_0,\ p_1 = q + z_1, \dots, p_{N-2} = q + z_{N-2}$, where $q$ is defined by (4.24) and all the quantities are generally assumed to be complex. Using these new notations, we can rewrite the generic term on the right-hand side of the previous equality as follows:

$$\begin{aligned}
&|A||p_0||p_1| \cdots |p_n| \left| \frac{p_{n+1} p_{n+2} - 2p_{n+1} + 1}{h^2} + k^2 p_{n+1} \right| \\
&\quad = |A||q + z_0||q + z_1| \cdots |q + z_n| \left| \frac{(q + z_{n+1})(q + z_{n+2}) - 2(q + z_{n+1}) + 1}{h^2} \right. \\
&\qquad\qquad \left. + k^2 (q + z_{n+1}) \right| \\
&\quad = |A||q + z_0||q + z_1| \cdots |q \\
&\qquad + z_n| \left| \underbrace{\frac{q^2 - 2q + 1}{h^2} + k^2 q}_{0} + \frac{z_{n+1} z_{n+2} + q(z_{n+1} + z_{n+2}) - 2z_{n+1}}{h^2} + k^2 z_{n+1} \right| \\
&\quad = |A||q + z_0||q + z_1| \cdots |q + z_n| \left| \frac{z_{n+2}(q + z_{n+1})}{h^2} + z_{n+1} \left( \frac{q-2}{h^2} + k^2 \right) \right| \\
&\quad = |A||q + z_0||q + z_1| \cdots |q + z_n| \left| \frac{z_{n+2}(q + z_{n+1})}{h^2} + \frac{z_{n+1}}{h^2} \mu \right|.
\end{aligned}$$

In the last chain of equalities, expression $\frac{q^2-2q+1}{h^2} + k^2 q$ turns into zero by virtue of the characteristic equation (4.23), and $\mu = q - 2 + k^2h^2$. Using the definition of $q$ from (4.24), we can obtain

$$|\mu|^2 = \left|-1 - \frac{1}{2}k^2h^2 - ikh\sqrt{1 - \frac{1}{4}k^2h^2} + k^2h^2\right| = \left|-1 + \frac{1}{2}k^2h^2 - ikh\sqrt{1 - \frac{1}{4}k^2h^2}\right|$$

$$= \left(-1 + \frac{1}{2}k^2h^2\right)^2 + k^2h^2\left(1 - \frac{1}{4}k^2h^2\right) = 1 - k^2h^2 + \frac{1}{4}k^4h^4 + k^2h^2 - \frac{1}{4}k^4h^4 = 1.$$

Finally, collecting all terms, we can now have

$$\begin{aligned}
&\sum_{n=0}^{N-1}\left|\frac{w_{n+1}^{(h)} - 2w_n^{(h)} + w_{n-1}^{(h)}}{h^2} + k^2 w_n^{(h)}\right| \\
&\quad = |A|\left|\frac{z_0}{h^2} + 2\frac{q-1}{h^2} + k^2\right| + |A|\left|\frac{z_1(q+z_0)}{h^2} + \frac{z_0}{h^2}\mu\right| \\
&\qquad + |A||q+z_0|\left|\frac{z_2(q+z_1)}{h^2} + \frac{z_1}{h^2}\mu\right| + |A||q+z_0||q+z_1|\left|\frac{z_3(q+z_2)}{h^2} + \frac{z_2}{h^2}\mu\right| + \cdots \\
&\qquad + |A||q+z_0||q+z_1|\dots|q+z_{N-3}|\left|\frac{z_{N-2}}{h^2}\mu\right| \\
&\quad \geq |A|\left|2\frac{q-1}{h^2} + k^2\right| - |A|\left|\frac{z_0}{h^2}\right| + |A|\left|\frac{z_0}{h^2}\right||\mu| - |A||q+z_0|\frac{|z_1|}{h^2} + |A||q+z_0|\frac{|z_1|}{h^2}|\mu| \\
&\qquad - |A||q+z_0||q+z_1|\frac{|z_2|}{h^2} + |A||q+z_0||q+z_1|\frac{|z_2|}{h^2}|\mu| - \cdots \\
&\qquad + |A||q+z_0||q+z_1|\dots|q+z_{N-3}|\frac{|z_{N-2}|}{h^2}|\mu| \\
&\quad = |A|\left|2\frac{q-1}{h^2} + k^2\right|.
\end{aligned}$$

In other words, we have obtained the inequality

$$\sum_{n=0}^{N-1}\left|\frac{w_{n+1}^{(h)} - 2w_n^{(h)} + w_{n-1}^{(h)}}{h^2} + k^2 w_n^{(h)}\right| \geq |A|\left|2\frac{q-1}{h^2} + k^2\right|. \tag{4.30}$$

To establish the result of the theorem, i.e., formula (4.29), it remains to show only that there will be a particular $w^{(h)} = w_n^{(h)}$ for which inequality (4.30) transforms into the equality. Clearly, the equality in formula (4.30) is achieved for $w_n^{(h)} = Aq^n$, $n \geq 0$, because in this case $z_0 = z_1 = \cdots = z_{N-2} = 0$. This completes the proof. ∎

Let us also recall that if we multiply the sum on the left-hand side of either formula (4.29) or formula (4.30) by the grid size $h$, we obtain the discrete $L_1$ norm of the control sources $g^{(h)}$. Therefore, inequality (4.30) transforms into

$$\left\|g^{(h)}\right\|_1 \geq \left|g_{\text{monopole}}^{(h,\,\text{surf})}\right| h, \tag{4.31}$$

and consequently, we have, in effect, demonstrated the global $L_1$ minimality of the surface control sources:

$$\min_{w^{(h)}} \left\|g^{(h)}\right\|_1 = \left|g_{\text{monopole}}^{(h,\,\text{surf})}\right| h. \tag{4.32}$$

Equality (4.32) is a one-dimensional counterpart of (4.15), but unlike the experimentally established formula (4.15), equality (4.32) has been proven rigorously.

The foregoing proof of Theorem 4.1 also reveals the mechanism of discrepancy between the optimal control $g^{(h,\,\mathrm{surf})}_{\mathrm{monopole}}$ and all other suboptimal controls. Namely, every time the auxiliary function $w_n^{(h)}$ "departs" from the pure right-traveling wave $Aq^n$, which is equivalent to having $z_n \neq 0$, we may pick up additional value of $\|g^{(h)}\|_1$ in case the actual estimate based on the triangle inequality that we use,

$$\begin{aligned}|A||q+z_0||q+z_1|\cdots|q+z_n|&\left|\frac{z_{n+2}(q+z_{n+1})}{h^2}+\frac{z_{n+1}}{h^2}\mu\right|\\ &\geq |A||q+z_0||q+z_1|\cdots|q+z_n|\frac{|z_{n+1}|}{h^2}|\mu|\\ &\quad -|A||q+z_0||q+z_1|\cdots|q+z_n||q+z_{n+1}|\frac{|z_{n+2}|}{h^2},\end{aligned}$$

happens to be "strictly greater" rather than "greater or equal" for this given term. It is also interesting to look into the role of the ABC (4.25). This boundary condition "swallows" the last term in the sum so that all the previous terms can cancel one another in pairs, and only the first term $|g^{(h,\,\mathrm{surf})}_{\mathrm{monopole}}|$ will remain.

Next, we will analyze the continuous case. Assume that $w(x)$ is a regular smooth function, which is defined on the interval $[0, X]$ and satisfies boundary conditions (4.19) and (4.22). Let us also assume that the grid function $w^{(h)} = w_n^{(h)}$, $n = 0, 1, \dots, N-1$, is the trace of $w(x)$ on the aforementioned uniform grid with size $h$: $w_n^{(h)} = w(x_n) \equiv w(n \cdot h)$. Note that we need to require sufficient smoothness of $w(x)$ in order to guarantee the consistency of the finite-difference scheme: $\boldsymbol{L}^{(h)}w^{(h)} = \boldsymbol{L}w + O(h^2)$ (see (4.16) and (4.17)). Let us additionally define $w_{-1}^{(h)} = qw_0^{(h)}$ and $w_N^{(h)} = qw_{N-1}^{(h)}$, in accordance with the boundary conditions (4.21) and (4.25), respectively, like in the formulation of Theorem 4.1. Then for small $h$ we can disregard the quadratic terms in the definition of $q$ (see (4.24)) and have for the right endpoint

$$\frac{w_N^{(h)} - w_{N-1}^{(h)}}{h} = -ikw_{N-1}^{(h)},$$

which is obviously an approximation of the continuous ABC (4.22) with the accuracy $O(h)$. Similarly, for the left endpoint we obtain

$$\frac{w_0^{(h)} - w_{-1}^{(h)}}{h} = ikw_0^{(h)},$$

which is an $O(h)$ accurate approximation of the second boundary condition (4.19) under the assumption that the field to be controlled is $u(x) = u^-(x) = Ae^{ikx}$, $x < 0$, and consequently, $\frac{du}{dx}\big|_{x=0} = iku(0)$. Altogether, we have constructed a grid function $w^{(h)} = w_n^{(h)}$, $n = -1, 0, \dots, N$, that satisfies the conditions of Theorem 4.1 and also approximates on the grid all the continuous requirements of the function $w = w(x)$.

Let us now again multiply both sides of inequality (4.30) by the positive quantity $h$ and consider independently the limit on its right-hand side and the limit on its left-hand side as $h \longrightarrow +0$. First, we obtain

$$|A|\left|2\frac{q-1}{h^2}+k^2\right|h = |A|\left|-k^2-\frac{2ik}{h}\sqrt{1-\frac{1}{4}k^2h^2}+k^2\right|h \longrightarrow 2|A|k \quad \text{as} \quad h \longrightarrow +0.$$

Note that the limit is equal to the magnitude of the surface monopole in the continuous formulation (see (4.27)). Next, on the left-hand side we have

$$\sum_{n=0}^{N-1}\left|\frac{w_{n+1}^{(h)}-2w_n^{(h)}+w_{n-1}^{(h)}}{h^2}+k^2w_n^{(h)}\right|h=\sum_{n=0}^{N-1}\left|\frac{d^2w}{dx^2}(x_n)+k^2w(x_n)\right|h+O(h^2)$$

$$\longrightarrow\int_0^X\left|\frac{d^2w}{dx^2}(x)+k^2w(x)\right|dx\qquad\text{as}\quad h\longrightarrow+0.$$

Note that the limit is equal to the $L_1$ norm $\|g\|_1$ of the continuous control sources $g(x)$ defined by formula (4.18). As inequality (4.30) holds for any given value of $h$, we can claim that it will also hold in the limit $h \longrightarrow +0$. Therefore, we have arrived at the following result.

COROLLARY 4.2. *Let a complex-valued function $w = w(x)$ be defined on $[0, X]$. Let $w(0) = A$, where $A \in \mathbb{C}$ is a given constant, and $w'(0) = ikw(0)$ and $w'(X) = -ikw(X)$. Then,*

$$\int_0^X\left|\frac{d^2w}{dx^2}(x)+k^2w(x)\right|dx\geq 2|A|k. \tag{4.33}$$

It is easy to see that the requirements of $w(x)$ formulated in Corollary 4.2 are equivalent to the conditions that guarantee the appropriateness of $w(x)$ for constructing the control sources $g(x)$ using (4.18); see formulae (4.19) and (4.22). Therefore, the result of Corollary 4.2, i.e., inequality (4.33), can be recast as

$$\|g\|_1\geq 2|A|k. \tag{4.34}$$

On the right-hand side of inequality (4.34) we have the magnitude of the "surface" monopole $g_{\text{monopole}}^{(\text{surf})}$ defined by formula (4.27). Note that, unlike in the previously considered discrete case, when the minimal solution $g_{\text{monopole}}^{(h,\,\text{surf})}$ of (4.28) was an element of the same class of control sources $g^{(h)}$ defined by (4.20), here the minimum $g_{\text{monopole}}^{(\text{surf})}(x)$ defined by (4.27) belongs to a different class of functions, namely, singular (i.e., $\delta$-type) distributions, as opposed to regular (i.e., $L_1^{(\text{loc})}$) distributions. In other words, $g_{\text{monopole}}^{(\text{surf})}(x) \notin L_1(\mathbb{R})$, and not even $L_1^{(\text{loc})}(\mathbb{R})$. As such, we cannot introduce the $L_1$ norm of $g_{\text{monopole}}^{(\text{surf})}(x)$. Therefore, inequality (4.34) formally has to stay the way it is. However, symbolically we can, of course, write

$$\int_{\mathbb{R}}\left|g_{\text{monopole}}^{(\text{surf})}(x)\right|dx=\int_{\mathbb{R}}|2Aik\delta(x)|\,dx=2|A|k, \tag{4.35}$$

which allows us to "informally" interpret inequality (4.34) as if $g_{\text{monopole}}^{(\text{surf})}(x)$ of (4.27) provided a lower bound in $L_1$ for all the control sources $g(x)$ defined by (4.18). Let us also note that "integration" with respect to $x$ in (4.35), which "removes" the $\delta$-function itself and leaves only its magnitude $2k|A|$, is a continuous analogue of multiplication by $h$ on the right-hand side of formulae (4.31) or (4.32). Therefore, we conclude that the continuous inequality (4.34) is a direct counterpart of the discrete inequality (4.31).

Even though $g_{\text{monopole}}^{(\text{surf})}(x) \notin L_1^{(\text{loc})}(\mathbb{R})$, we will still show that there are regular control sources $g(x) \in L_1^{(\text{loc})}(\mathbb{R})$ that are arbitrarily close to $g_{\text{monopole}}^{(\text{surf})}(x)$ in the weak sense. More precisely, we will construct a sequence of regular auxiliary functions $w_\epsilon(x)$ such that the corresponding $g_\epsilon(x)$ obtained according to (4.18) will converge to $g^{(\text{surf})}_{\text{monopole}}(x)$ of (4.27) in the sense of distributions. This will allow us to claim that although the minimal solution $g^{(\text{surf})}_{\text{monopole}}(x)$ is singular, it is, in fact, "on the borderline" of the class of regular solutions. In other words, it is a limiting point, in the sense of weak convergence, of the space of all $g(x)$ defined by formula (4.27). In addition, we will also show that the $L_1$ norms $\|g_\epsilon\|$ converge to the magnitude $2k|A|$ of the "surface" monopole $g^{(\text{surf})}_{\text{monopole}}(x)$ of (4.27). This will allow us to formulate in the continuous case the result similar to the minimality (4.32) but in the sense of "infimum" rather than "minimum."

Consider a regular function $w_\epsilon = w_\epsilon(x)$ that is defined on $[0, X]$ and satisfies boundary conditions (4.19) and (4.22) with $u(x) = Ae^{ikx}$ for $x < 0$. In addition, let us assume that not only for $x > X$, but also in between some (small) $\epsilon < X$ and $X$, the function $w_\epsilon(x)$ already coincides with a right-traveling wave: $w_\epsilon(x) = w_\epsilon(\epsilon)e^{-ik(x-\epsilon)}$, $\epsilon \le x \le X$. In other words, we require that $w_\epsilon(0) = A$, $w'_\epsilon(0) = ikA$, and $w'_\epsilon(\epsilon) = -ikw_\epsilon(\epsilon)$. For the purpose of obtaining the aforementioned convergent sequence, we will subsequently let $\epsilon \longrightarrow +0$. The control sources $g_\epsilon(x)$ are defined according to formula (4.18): $g_\epsilon(x) = -w''_\epsilon(x) - k^2 w_\epsilon(x)$, $0 \le x \le \epsilon$, and for $x > \epsilon$ we have $g_\epsilon(x) = 0$. If $\varphi = \varphi(x)$ is a test function on $\mathbb{R}$, i.e., a compactly supported infinitely smooth function (see [24]), then the corresponding functional, i.e., the distribution $g_\epsilon$ itself, can be represented as follows:

$$(g_\epsilon, \varphi) = \int_{\mathbb{R}} g_\epsilon(x)\varphi(x)dx = \int_0^\epsilon [-w''(x) - k^2 w(x)]\varphi(x)dx$$
$$= w(\epsilon)\varphi'(\epsilon) - w(0)\varphi(0) - [\varphi(\epsilon)w'(\epsilon) - \varphi(0)w'(0)] + \int_0^\epsilon [-w(x)\varphi''(x) + k^2 w(x)\varphi(x)]dx.$$

As $w(x) \in L_1^{(\text{loc})}(\mathbb{R})$ and $\varphi(x)$ is a test function, the integral on the right-hand side of the previous equality vanishes as $\epsilon \longrightarrow +0$. Let us now additionally assume that the functions $w_\epsilon = w_\epsilon(x)$ are constructed so that $w_\epsilon(\epsilon) \longrightarrow w_\epsilon(0)$ when $\epsilon \longrightarrow +0$. In other words, we assume continuity at $x = 0$. Then, because of the boundary condition (4.22) at $x = \epsilon$, we have $w'_\epsilon(\epsilon) \longrightarrow -ikA$ as $\epsilon \longrightarrow +0$. Altogether, we obtain

$$(g_\epsilon, \varphi) \longrightarrow 2ikA\varphi(0) \quad \text{as} \quad \epsilon \longrightarrow +0. \tag{4.36}$$

The limit (4.36) implies that in the sense of distributions

$$g_\epsilon(x) \longrightarrow g^{(\text{surf})}_{\text{monopole}}(x) \equiv 2ikA\delta(x) \quad \text{as} \quad \epsilon \longrightarrow +0. \tag{4.37}$$

Let now specify a particular form of $w_\epsilon(x)$:

$$w_\epsilon(x) = \frac{-ikA}{\epsilon}x^2 + ikAx + A, \qquad x \in [0, \epsilon]. \tag{4.38}$$

For this function, we have $w_\epsilon(0) = w_\epsilon(\epsilon) = A$, $w'_\epsilon(0) = ikA$, and $w'_\epsilon(\epsilon) = -ikA$, and consequently, $w_\epsilon(x)$ of (4.38) meets all the previous conditions. For the $L_1$ norm of the corresponding control $g_\epsilon(x)$, we obtain

$$\|g_\epsilon\|_1 = \int_0^\epsilon |w''_\epsilon(x) + k^2 w_\epsilon(x)|dx = \int_0^\epsilon |A| \left[k^2 + \left(-\frac{k^3}{\epsilon}x^2 + k^3 x - \frac{2k}{\epsilon}\right)^2\right]^{1/2} dx.$$

As we always have $0 \leq x \leq \epsilon$, the dominant term in the last integral for small $\epsilon$ is $\frac{2k}{\epsilon}$, and therefore

$$\|g_\epsilon\|_1 \longrightarrow 2k|A| \quad \text{as} \quad \epsilon \longrightarrow +0. \tag{4.39}$$

Putting together the result of Corollary 4.2 with the limits (4.37) and (4.39), we arrive at the following result.

THEOREM 4.3. *Let a complex-valued function $w = w(x)$ be defined on $[0, X]$. Let $w(0) = A$, where $A \in \mathbb{C}$ is a given constant, and $w'(0) = ikw(0)$ and $w'(X) = -ikw(X)$. Then, in the class of regular control sources $g(x)$ defined by formula* (4.18) *for all such $w(x)$, one can identify a sequence $g_\epsilon(x)$ that would converge in the sense of distributions to the point monopole $g^{(\text{surf})}_{\text{monopole}}(x)$ defined by formula* (4.27):

$$g_\epsilon(x) \longrightarrow g^{(\text{surf})}_{\text{monopole}}(x) \equiv 2ikA\delta(x) \quad \text{as} \quad \epsilon \longrightarrow +0.$$

*Besides, the magnitude of the point monopole $g^{(\text{surf})}_{\text{monopole}}(x)$ of* (4.27) *provides the greatest lower bound for $L_1$ norms of all the control sources $g(x)$ of* (4.18):

$$\inf_{w(x)} \|g\|_1 = 2k|A|. \tag{4.40}$$

Clearly, estimate (4.40) can be interpreted as global $L_1$ minimality of the "surface" control (4.27) among the continuous one-dimensional control sources (4.18). It is a continuous version of the previously established discrete result (4.32).

**5. Discussion.** For the problem of active control of sound, we have systematically described time-harmonic general solutions for the volume and surface control sources in the continuous and discrete formulation of the problem. These control sources guarantee the identical cancellation of unwanted noise on a predetermined region of interest. We have also proposed a criterion for optimization of the resulting control sources. This criterion chooses the overall absolute acoustic source strength as the cost function for minimization, and as such admits a clear physical interpretation. Mathematically, it translates into minimization of complex-valued functions in the sense of $L_1$, which is a very challenging problem from the standpoint of numerical implementation. We have still managed, though, to compute several two-dimensional numerical solutions using the algorithm SeDuMi. All these solutions demonstrate a coherent behavior—the minimum is achieved on the surface of the protected region. In other words, the minimum is delivered by the appropriate surface monopole controls. Therefore, the numerical evidence that we have received indicates that surface monopoles may provide a global $L_1$ minimum for the control sources in the general setting. We have been able to rigorously prove this result in the one-dimensional case for both continuous and discrete formulation of the problem. Even though we have not yet been able to prove a similar result for a general multi-dimensional framework, we still believe that it is true, because a combination of the two-dimensional numerical evidence and a one-dimensional accurate proof cannot, in our opinion, be a mere coincidence. Therefore, we put forward the minimization result in the form of a conjecture. Let us recall that according to (2.30) the surface monopole controls are given by

$$g^{(\text{surf})}_{\text{monopole}}(\boldsymbol{x}) = -\left[\frac{\partial w}{\partial \boldsymbol{n}} - \frac{\partial u}{\partial \boldsymbol{n}}\right]_\Gamma \delta(\Gamma) = -\left[\frac{\partial \tilde{w}}{\partial \boldsymbol{n}} - \frac{\partial u^-}{\partial \boldsymbol{n}}\right]_\Gamma \delta(\Gamma) \equiv \nu(\boldsymbol{x})|_{\boldsymbol{x}\in\Gamma} \cdot \delta(\Gamma), \tag{5.1}$$

where $\tilde{w}(x) = w(\boldsymbol{x}) - u^+(\boldsymbol{x})$, as before, and $w(\boldsymbol{x})$ is a solution to the exterior Dirichlet problem (2.23). Then, we can formulate the following.

CONJECTURE 5.1. *Let a complex-valued function $w = w(\boldsymbol{x})$ be defined on $\Omega_1 = \mathbb{R}^n \backslash \Omega$, and let it be sufficiently smooth so that the operator $\boldsymbol{L}$ of* (1.1) *can be applied to $w(\boldsymbol{x})$ on its entire domain in the classical sense, and the result $\boldsymbol{L}w$ can be locally absolutely integrable. Let, in addition, $w(\boldsymbol{x})$ satisfy the interface conditions* (2.2), *where $u = u(\boldsymbol{x})$ is a given field to be controlled, and the appropriate Sommerfeld radiation boundary conditions at infinity,* (1.2a) *or* (1.2b). *Then the greatest lower bound for the $L_1$ norms of all the control sources $g(\boldsymbol{x})$ obtained with such auxiliary functions $w(\boldsymbol{x})$ using formula* (2.1) *is given by the $L_1$ norm on $\Gamma$ of the magnitude of surface monopoles* (5.1):

$$\inf_{w(\boldsymbol{x})} \int_{\Omega_1} |g(\boldsymbol{x})| d\boldsymbol{x} = \int_{\Gamma} |\nu(\boldsymbol{x})| ds. \tag{5.2}$$

Alternatively, we can rewrite (5.2) as

$$\inf_{w(\boldsymbol{x})} \|g(\boldsymbol{x})\|_{1,\Omega_1} = \|\nu\|_{1,\Gamma}. \tag{5.3}$$

Equality (5.3) is a multidimensional generalization of (4.40). Let us also notice that equality (4.15), which was obtained on the basis of experimental observations in two space dimensions, can be considered a discrete two-dimensional prototype of (5.3).

In the formulation of Conjecture 5.1, we did not include the results on the convergence of a sequence of volumetric controls to the surface layer $\nu\delta(\Gamma)$ (see (5.1)) and on the convergence of the corresponding $L_1$ norms, as we did in Theorem 4.3 for the one-dimensional case. We believe, though, that these results can be easily formulated and justified in the multidimensional framework using an approach similar to the one that we have used in the one-dimensional case. The key missing part, however, that does not yet allow us to transform Conjecture 5.1 into a theorem, is proving that surface monopoles provide *a lower bound* for the volumetric controls in the sense of $L_1$, whereas showing that this is the greatest lower bound is more straightforward. The analysis of this problem will be a subject of our future research. In this connection we can mention only that, at least in the two-dimensional case, the geometry of the protected region $\Omega$ should not be a limitation when constructing a general proof. If one can prove the result for a constant-width linear strip with periodic boundary conditions on its sides, and with the interface $\Gamma$ being a segment of the straight line normal to the sides of the strip, then for any other shape the same result can likely be obtained with the help of a conformal mapping.

**Acknowledgments.** It is our pleasure to acknowledge most useful discussions with Jan Hesthaven, Wu Li, Michael Overton, and Victor Ryaben'kii. We would also like to thank the reviewer of the paper, who drew our attention to several important points and thereby helped make the revised manuscript a substantial improvement over its original version.

## REFERENCES

[1] K. D. ANDERSEN, E. CHRISTIANSEN, A. R. CONN, AND M. L. OVERTON, *An efficient primal-dual interior-point method for minimizing a sum of Euclidean norms*, SIAM J. Sci. Comput., 22 (2000), pp. 243–262.

[2] A. P. CALDERON, *Boundary-value problems for elliptic equations*, in Proceedings of the Soviet-American Conference on Partial Differential Equations, Novosibirsk, Moscow, 1963, Fizmatgiz, Moscow, pp. 303–304.

[3] S. J. Elliot, *Signal Processing for Active Control*, Academic Press, San Diego, 2001.
[4] G. Fibich and S. V. Tsynkov, *High-order two-way artificial boundary conditions for nonlinear wave propagation with backscattering*, J. Comput. Phys., 171 (2001), pp. 632–677.
[5] C. R. Fuller, S. J. Elliot, and P. A. Nelson, *Active Control of Vibration*, Academic Press, London, 1996.
[6] J. Lončarić, *Sensor/actuator placement via optimal distributed control of exterior Stokes flow*, in Computational Methods in Optimal Design and Control: Proceedings of the AFOSR Workshop on Optimal Design and Control, J. T. Borggaard, J. Burns, E. Cliff, and S. Schreck, eds., Progr. Systems Control Theory 24, Birkhäuser Boston, Cambridge, MA, 1998, pp. 303–322.
[7] J. Lončarić, V. S. Ryaben'kii, and S. V. Tsynkov, *Active shielding and control of noise*, SIAM J. Appl. Math., 62 (2001), pp. 563–596.
[8] J. Lončarić and S. V. Tsynkov, *Optimization of Power in the Problems of Active Control of Sound*, manuscript, 2003.
[9] J. Lončarić and S. V. Tsynkov, *Quadratic Optimization in the Problems of Active Control of Sound*, Technical report 2002-35, NASA/CR-2002-211939, ICASE, Hampton, VA, 2002 (also SIAM J. Appl. Math., submitted).
[10] C. L. Morfey, *Dictionary of Acoustics*, Academic Press, San Diego, 2001.
[11] P. A. Nelson and S. J. Elliot, *Active Control of Sound*, Academic Press, San Diego, 1999.
[12] Y. Nesterov and A. Nemirovskii, *Interior-Point Polynomial Algorithms in Convex Programming*, SIAM Stud. Appl. Math. 13, SIAM, Philadelphia, 1994.
[13] Y. Nesterov and M. J. Todd, *Self-scaled barriers and interior-point methods for convex programming*, Math. Oper. Res., 22 (1997), pp. 1–42.
[14] T. W. Roberts, D. Sidilkover, and S. V. Tsynkov, *On the combined performance of nonlocal artificial boundary conditions with the new generation of advanced multigrid flow solvers*, Computers and Fluids, 31 (2001), pp. 269–308.
[15] V. S. Ryaben'kii, *Method of Difference Potentials and Its Applications*, Springer-Verlag, Berlin, 2002.
[16] R. T. Seeley, *Singular integrals and boundary value problems*, Amer. J. Math., 88 (1966), pp. 781–809.
[17] J. F. Sturm, *Using SeDuMi* 1.02, *A MATLAB toolbox for optimization over symmetric cones*, Optim. Methods Softw., 11–12 (1999), pp. 625–653; special issue on interior point methods (CD supplement with software).
[18] A. N. Tikhonov and A. A. Samarskii, *Equations of Mathematical Physics*, Pergamon Press, Oxford, 1963.
[19] S. V. Tsynkov, *Numerical solution of problems on unbounded domains. A review*, Appl. Numer. Math., 27 (1998), pp. 465–532.
[20] S. V. Tsynkov, *On the definition of surface potentials for finite-difference operators*, J. Sci. Comput., 18 (2003), pp. 155–189.
[21] R. J. Vanderbei, *Linear Programming: Foundations and Extensions*, Kluwer Academic Publishers, Boston, 2001.
[22] R. I. Veizman and V. S. Ryaben'kii, *Difference problems of screening and simulation*, Dokl. Akad. Nauk, 354 (1997), pp. 151–154.
[23] R. I. Veizman and V. S. Ryaben'kii, *Difference simulation problems*, Trans. Moscow Math. Soc., 58 (1997), pp. 239–248.
[24] V. S. Vladimirov, *Equations of Mathematical Physics*, Dekker, New York, 1971.
[25] Y. Ye, M. J. Todd, and S. Mizuno, *An $O(\sqrt{n}L)$-iteration homogeneous and self-dual linear programming algorithm*, Math. Oper. Res., 19 (1994), pp. 53–67.